Two-phase flow through porous media in the fixed-contact-line regime

S. R. Pride
Université de Rennes 1, Géosciences Rennes, Campus Beaulieu Bâtiment 15, 35042 Rennes Cedex, France

E. G. Flekkøy
Department of Physics, University of Oslo, P.O. Box 1048 Blindern, 0316 Oslo 3, Norway
(Received 17 March 1999; revised manuscript received 24 May 1999)

The complete set of equations controlling immiscible two-phase flow through porous media are derived from first principles under the sole restriction that contact lines between the two fluids and the grain surfaces are not allowed to migrate irreversibly. Because rough grain surfaces have the ability to trap contact lines over significant ranges of capillary-pressure variation, such laws are of practical interest. As distinct from previous coarse-graining work, we explicitly allow for the stretching of the fluid interface, which results in considerable nonlinearity at the macroscopic scale. The laws are obtained through an asymptotic analysis and have several new features compared to the standard laws conventionally used in two-phase flow modeling. These include the need to (i) distinguish between measurable fluxes and the volume-averaged flow; (ii) allow for flow induced by the time rate of change of the capillary pressure; and (iii) include quadratic-force terms in the generalized Darcy laws when macroscopic-pressure diffusion is slow (as defined herein).
[S1063-651X(99)01510-X]

PACS number(s): 81.05.Rm, 47.55.Kf, 47.55.Mh, 47.10.+g

I. INTRODUCTION

Despite their economic importance, the macroscopic laws controlling immiscible two-phase flow through porous materials such as sedimentary rock remain poorly understood. The reason for this is that the fluid distributions in a sample change whenever the forces driving the flow change. Since the fluid distributions define the resistance experienced by each fluid, the transport laws controlling the macroscopic (volume-averaged) flux are, in general, nonlinear and history-dependent functions of the applied force.

Furthermore, when the saturation levels are changing, it is conventional to complete the macroscopic-flow description with a relation between the average capillary pressure P_c in each sample and the saturation φ [1–3]. The $P_c(\varphi)$ relation is often taken from static fluid-invasion experiments in which neither fluid forms a connected path across the sample. It is then applied to flow situations where both fluids percolate. Such inconsistent use of $P_c(\varphi)$ is common practice even to this day.

In the present work, we wish to establish a consistent macroscopic two-phase flow description that connects to the pore-scale physics in a well-defined way. To do so, analysis is limited to the flow regime where history dependence is not important. Such a regime has two requirements: (i) both fluids percolate in the absence of flow, and (ii) contact lines between the fluid interface and grain surfaces remain fixed once forces are applied and flow begins. The hysteresis of contact-line movement [4] is behind the need for both of these requirements. As will be shown, grains with rough surfaces have the ability to pin contact lines over nontrivial ranges of applied force.

We view our contribution as a practical first step toward a more general model in which larger applied-force variations are allowed for so that contact lines may irreversibly migrate. Unfortunately, there remains much uncertainty associated with the proper continuum boundary conditions near moving contact lines (see [5] for a review). Starting from the pore scale, we underline that, to our knowledge, no work has ever attempted to obtain the macroscopic flow laws when contact lines are free to redistribute.

The standard formulation [1] has three parts: (i) the conservation of mass of both fluids; (ii) a Darcy law for each fluid; and (iii) an assumed macroscopic capillary-pressure law $P_c(\varphi)$. When there is a large viscosity contrast between the two fluids such as for air and water, it is common to make the additional assumptions that the two Darcy laws are decoupled and that the air does not move at the macroscale (which leads to the so-called Richard's equation). Such formulations give a closed set of equations that, along with stated boundary conditions, are used to make predictions of how fluid saturation and pressure evolve through time in the earth. However, the formulation has never been justified through coarse-graining of the pore-scale physics. Inconsistencies in the scheme have been voiced [7] and a central purpose of this paper is to put the formulation through a careful examination.

In the present work, saturation variations are allowed for by allowing the fluid interface to stretch. The important role played by saturation gradients is emphasized. The analysis shows how the usual linear transport laws yield to nonlinear forcing at finite capillary number ϵ. The linear Darcy laws emerge as $\epsilon \to 0$. At this order it is shown that the cross-coupling terms satisfy Onsager reciprocity—a result which is obtained in the context of statistical mechanics in a companion paper [6].

Existing coarse-graining work for this problem includes that of Whitaker [8] and Auriault [9,10]. These authors also restrict analysis to the case of fixed contact lines. However, neither treat the important role played by the fluid-interface deformation as a function of applied-force levels. Thus, neither work resolves any of the questions surrounding the use

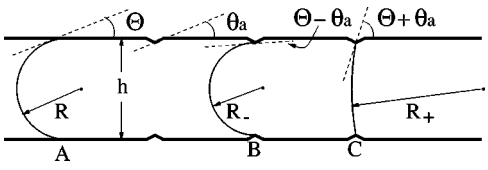

FIG. 1. A fluid channel with small asperities characterized by an angle θ_a and negligible height.

of $P_c(\varphi)$ nor considers the nature of any nonlinearity in the flow description. From a technical viewpoint, our work is able to go beyond this existing work because we explicitly treat the interface displacement.

II. ASSUMPTIONS

Before stating the specific pore-scale boundary value problem that will be used to obtain the macroscopic laws, we wish to discuss some of the assumptions that go into the model. At the scale of the porous continuum, the only exact statement that can be made is the conservation of mass of the two fluids. The remaining laws require approximations and assumptions that at the very least should be clearly stated and internally consistent and would preferably be associated with some kind of validity condition.

A. Fixed contact lines

We begin with a simple qualitative justification for the principal approximation of this (and the other existing) coarse-graining work; namely, that contact lines between the two fluids and the grains can remain fixed as applied forces vary. Is such a flow regime even possible?

Roughness of the solid walls is known to provide one mechanism for contact-line hysteresis [4]. This mechanism is illustrated in Fig. 1, which shows a pore channel with a few asperities representing the surface roughness. In a channel with flat walls, the contact angle Θ determines the equilibrium curvature of a meniscus (such as meniscus A in the figure) and thus the local capillary pressure $\mathcal{P}_c$. If the capillary pressure were to deviate a small amount from this value due to externally applied pressures, a meniscus would spontaneously migrate to the right (for a decrease in $\mathcal{P}_c$) or to the left (for an increase) until an asperity was encountered. Upon encountering an asperity, the contact lines of a left-moving meniscus will spontaneously rise up the asperity face, reach the peak, and just as they start to descend they will find the equilibrium contact angle and stop. On the pore scale, the peaks take the form of sharp edges, so the meniscus stops (becomes trapped) essentially right on the edge. If the pressure drop increases further, a meniscus (such as B in the figure) will bulge while its contact lines remain fixed to the edge until finally its curvature is reduced to where it may descend to the left at the proper contact angle. Similar things can be said for a right-moving meniscus except that the external pressure drop must be lowered and the meniscus (such as C in the figure) must become more flat in order to overcome the asperity trap and descend to the right with the proper contact angle. Thus, all meniscii become trapped on asperity edges and can tolerate a certain range of $\mathcal{P}_c$ variation before they migrate away. We now estimate this range.

On a flat wall the equilibrium value of the interface curvature is $1/R = 2\cos\Theta/h$, where h is the channel width. This yields the well-known value for the pressure drop

$$\mathcal{P}_c = \frac{2\sigma}{h}\cos\Theta, \tag{1}$$

where σ is the surface tension. At the asperities, the wall is tilted by an angle θ_a as shown in the figure so that the wall orientation of the meniscii is tilted by the same angle relative to the meniscii on the flat wall. This means that the equilibrium curvature on the left-facing side of an asperity is $1/R_- = 2\cos(\Theta-\theta_a)/h$ while that on the right-facing side is $1/R_+ = 2\cos(\Theta+\theta_a)/h$. Hence, for meniscii on the edges, $\mathcal{P}_c$ can be in the range

$$\frac{2\sigma\cos(\Theta+\theta_a)}{h} \leqslant \mathcal{P}_c \leqslant \begin{cases} 2\sigma\cos(\Theta-\theta_a)/h & \text{if } \Theta > \theta_a \\ 2\sigma/h & \text{if } \Theta < \theta_a . \end{cases} \tag{2}$$

The reason for the two possible upper limits is that if $\Theta < \theta_a$, then once we arrive at $\mathcal{P}_c = 2\sigma/h$, the curvature is at its smallest possible value $R_- \approx h/2$ so that any further increase in the capillary pressure would cause the meniscus to break off from the wall.

The meniscii B and C in Fig. 1 correspond to the high and low values of the range (2). For a trapped meniscus to move to the right, the external pressure drop must be lower than the lowest $\mathcal{P}_c$ value, while for a meniscus to move to the left, the external pressure must be higher than the high value of $\mathcal{P}_c$. The fact that these pressures are different is an important source of hysteresis.

So a meniscus that entered a channel of width h at a capillary pressure close to the equilibrium value of Eq. (1) will remain trapped on an asperity within the channel until the order-of-magnitude deviations $\Delta\mathcal{P}_c$ of the capillary pressure exceed the range

$$-\sigma/h < \Delta\mathcal{P}_c < +\sigma/h. \tag{3}$$

This range is nontrivial especially in tight materials like rock. For an oil/water meniscus ($\sigma = 5\times10^{-2}$ Pa m) trapped in a 5-micron channel (a sandstone), the condition is -10^4 Pa$< \Delta\mathcal{P}_c <+10^4$ Pa. Note that 10^4 Pa is the pressure produced by a one-meter stand of water or a standard household vacuum cleaner.

Of course, there is a wide distribution of pore widths h in real rocks. For an externally fixed value of $\mathcal{P}_c$, we may expect that a small but finite number of the meniscii throughout a sample are just at the end of the range (2) so that any local perturbations in the capillary pressure may lead to spontaneous motion of the contact lines. This is always true and in this sense our coarse-graining effort can only be considered approximate. Nonetheless, the majority of meniscii will be stuck on asperities at pressures well within the range (2).

B. Applied forces

We imagine an initial state in which no flow is occurring. Forces are then applied and flow begins. The purpose of this

subsection is to identify these applied forces as gradients of the average pressures in each sample (or averaging volume).

Our initial state is defined by both fluids having continuous paths across each sample and by the fluids being everywhere stationary. In this state, gravity alone is generating the pressure distributions and the fluids have adjusted their meniscii (all trapped on asperities) to accommodate the pore-scale capillary pressure (we label the two fluids as a and b throughout the entire paper),

$$P_c^o(\mathbf{r}) = \mathcal{P}_a - \mathcal{P}_b + (\rho_b - \rho_a)\mathbf{g}\cdot\mathbf{r}, \tag{4}$$

where $\mathbf{g}$ is the acceleration of gravity, $\mathbf{r}$ is the distance vector, and ρ_a and ρ_b are the fluid densities. The constant difference $\mathcal{P}_a - \mathcal{P}_b$ is thus the capillary pressure at the arbitrarily selected origin.

To get flow, pressure gradients must be applied. In the earth, for example, we might inject or extract fluids at selected places. If flow is occurring in an averaging volume somewhere (possibly far removed from the injection/extraction points), the fluids experience applied pressures that are different on one side of the volume as compared to the other. In general, the pressure drop of fluid a across the volume will be different from that of fluid b. These pressure drops are the macroscopic pressure gradients in the theory. The injection process will also change the average pressure in each sample and both effects must be properly allowed for.

To fix a concrete image, imagine an averaging volume that is in the form of a flat slab, say a circular disk with radius much greater than thickness L so that only the boundary conditions on the flat faces need to be worried about. The disk is oriented so that the maximum pressure drops are parallel with the axis coordinate s. If this disk truly corresponds to a region within the earth (and not a laboratory sample), then the applied-pressure boundary conditions on the flat faces $s = \pm L/2$ can be written ($f = a$ or b)

$$p_f(\mathbf{r}) = \begin{cases} \overline{p_f} + \Delta P_f/2 + \pi_f^+(\mathbf{r}), & s = +L/2 \\ \overline{p_f} - \Delta P_f/2 + \pi_f^-(\mathbf{r}), & s = -L/2, \end{cases} \tag{5}$$

where

$$\overline{p_f} = \frac{1}{V_f}\int_{\Omega_f} p_f dV \tag{6}$$

is the average pressure throughout the portion Ω_f of the averaging volume occupied by fluid f. The ΔP_f are the average pressure drops across the disk so that the functions $\pi_f^{\pm}(\mathbf{r})$ are the spatial deviations created by pore-scale details of the flow process and which average to zero on each disk face.

We now make the assumption that the average flow in an averaging volume is unaffected by the presence of the $\pi_f^{\pm}(\mathbf{r})$ on the disk faces. These flow-induced deviations play an important role within the sample and must be modeled there so that the incompressible flow may accelerate and decelerate through constrictions. Our assumption is that taking their boundary values to be zero on the disk faces will not affect the average flow.

This assumption could be formally justified using Green's functions and the notion that the fluids are multiply connected throughout a sample. The qualitative idea is that a given value of $\pi_f^+(\mathbf{r})$ (say positive) in some pore on $s = +L/2$ has an influence at an interior point that (i) falls off with distance from the interface, and (ii) is at least partially canceled by a negative value coming from some other pore on $s = +L/2$. Thus, for sufficiently thick samples and for sufficiently connected fluids (so that a given interior point is connected to many pores on the disk face without crossing any meniscii) we believe it is evident that the assumption can be formally justified and we do not pause to do so here. In passing, one may note that if this assumption were not valid, then standard laboratory flow experiments (in which $\pi_f^{\pm} = 0$) would be meaningless for applications to earth problems.

The local (applied) pressure at every point within a sample can thus be written

$$p_f(\mathbf{r}) = \overline{p_f} + \frac{\Delta P_f}{L}s + \pi_f(\mathbf{r}) \tag{7}$$

so that the local (applied) pressure gradient is

$$\nabla p_f(\mathbf{r}) = \frac{\Delta P_f}{L}\hat{\mathbf{s}} + \nabla \pi_f(\mathbf{r}) \tag{8}$$

and our assumption is the boundary condition

$$\pi_f(\mathbf{r}) = \begin{cases} 0, & s = +L/2 \\ 0, & s = -L/2. \end{cases} \tag{9}$$

Thus, the applied forces (due to the distant injection process) can be modeled within each sample as uniform force densities

$$\mathbf{F}_f = -\frac{\Delta P_f}{L}\hat{\mathbf{s}}. \tag{10}$$

In order to obtain a theory that lets the material properties of the earth (as well as the distant injection event) fix the values of $\mathbf{F}_f$ acting in each averaging volume, we must next connect these forces to gradients of the average fluid pressures.

This last step is done using the definition of the derivative of a volume-averaged quantity [8,11]

$$\nabla(\varphi_f \overline{p_f}) = \frac{1}{V}\int_{\partial E_f} \mathbf{n} p_f dS, \tag{11}$$

where φ_f is the volume fraction of each fluid,

$$\varphi_f(\mathbf{r}) = \frac{1}{V}\int_{\Omega_f} dV = \frac{V_f(\mathbf{r})}{V}, \tag{12}$$

and where ∂E_f is the portion of the exterior surface of the averaging volume occupied by fluid f and having normal $\mathbf{n}$. The saturation gradient is defined

$$\nabla \varphi_f = \frac{1}{V}\int_{\partial E_f} \mathbf{n} dS \tag{13}$$

and thus exists when there is more fluid-f surface area on one side of a sample as compared to the other.

For our case of an averaging disk, if the boundary conditions (5) and (9) are used in the definition (11), we obtain

$$\hat{\mathbf{s}}\cdot\boldsymbol{\nabla}(\varphi_f\overline{p_f})=\overline{p_f}\hat{\mathbf{s}}\cdot\boldsymbol{\nabla}\varphi_f+\frac{\Delta P_f}{L}\Phi_f, \tag{14}$$

where the saturation gradient is

$$\hat{\mathbf{s}}\cdot\boldsymbol{\nabla}\varphi_f=\frac{A_f^+-A_f^-}{AL} \tag{15}$$

and where Φ_f is an external-area measure of saturation

$$\Phi_f=\frac{A_f^++A_f^-}{2A}. \tag{16}$$

Here, the $A_f^{\pm}$ are the total areas of fluid f on the disk faces $s=\pm L/2$ while A is the area of each disk face.

From Eq. (14), it follows that for arbitrary disk orientations

$$\varphi_f\boldsymbol{\nabla}\overline{p_f}=\Phi_f\frac{\Delta P_f}{L}\hat{\mathbf{s}}. \tag{17}$$

In the following, we assume that

$$\Phi_f\cong\varphi_f. \tag{18}$$

Imagine that an averaging disk is sliced parallel to its two end faces at many points along its length. The area saturation A_f/A is then measured on each slice. The condition for Eq. (18) to be a valid estimate of Φ_f is that such slice saturations must scatter about the straight line connecting the end-face values A_f^+/A and A_f^-/A. Sedimentary rock will typically satisfy this constraint. One must have large nonsystematic variations of the porosity (e.g., voids that cluster on one side of a sample relative to the other) before this assumption breaks down.

Thus, we may finally write the principal result of this section,

$$\mathbf{F}_f=-\boldsymbol{\nabla}\overline{p_f}. \tag{19}$$

In other words, any injection/extraction process that results in flow is associated with uniform-force densities acting on the fluids in each averaging volume and such forces can be identified as the macroscopic gradient in the average applied pressures. It is the purpose of the macroscopic theory to provide rules for how these $\overline{p_f}$ are distributed through space and time.

C. Connection to invasion problems

We finally discuss how the theory developed in this paper is to be used in the context of a typical three-dimensional (3D) invasion problem. These comments are essential in order to understand the goals of the subsequent analysis.

Imagine a situation where fluid *a* is being injected from a well into an earth initially saturated with fluid *b*. There might also be a second well some distance away in which fluid *b* is being extracted. If the injection/extraction is stopped after fluid *a* has invaded only a small distance into the formation, there will be a macroscopic invasion front separating a region of partial saturation from the region completely saturated by fluid *b*. The topological nature of this macroscopic invasion front (e.g., whether it has a fractal dimension greater than the Euclidean dimension of 2) is a function of the nature of the invasion experiment as will be briefly discussed below.

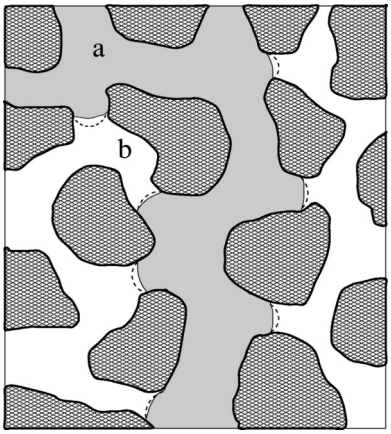

FIG. 2. A saturation state in a small pixel well behind the macroscopic invasion front. Fluid *a* is the nonwetting invading fluid. The meniscii in a state of no applied pressure gradients are denoted with solid lines while the meniscii once the drainage is established are shown as dashed lines.

For modeling purposes, we now discretize the earth into 3D pixels. Each pixel represents an averaging volume or ''sample'' as discussed in the preceding section. We can distinguish between three types of pixels: (i) pixels interior to the macroscopic front in which both fluids percolate, (ii) pixels exterior to the front that are entirely saturated by fluid *b*, and (iii) boundary pixels that contain within them the macroscopic front.

If injection were to resume at sufficiently low rates, the laws that we propose in this paper would be capable of modeling the flow everywhere throughout the region of interior pixels. However, the boundary pixels are experiencing contact-line movement and thus obey different laws. Thus, the macroscopic front represents a special boundary condition surrounding the interior region where our theory applies. We will not consider here the nature of these invasion-front boundary conditions, but they are the key quantities that define the saturation and saturation gradient of the two-phase transport backbones being formed within the boundary pixels. Once the initial saturation and saturation gradient are laid down in a pixel, subsequent saturation variations (the ones modeled in this paper) will be dominated by stretching of the meniscii with contact lines remaining fixed, as is depicted in Fig. 2. Thus, the theory of this paper is providing the rules for how the invading fluid arrives at the evolving macroscopic invasion front.

To justify this image of the invasion process, we make connection with the 3D drainage experiments of Frette *et al.* [12]. These authors inject a nonwetting fluid at a fixed point within a 3D porous material that is initially saturated with wetting fluid. They visually monitor how the saturation structure develops around the injection point and observe that such structure is a function of the injection rate. At very low injection rates (capillary number $\epsilon\ll 10^{-4}$), an irregular

fractal structure develops, while at higher rates ($\epsilon \gtrsim 10^{-4}$), a much more regular ball-like structure is observed. But even for the uniform ball structure, the invading fluid occupies less than half the pore space of the interior region so that the interior pixels are all traversed by both fluids.

This dependence on injection rate can be understood as follows. At sufficiently low rates, there will always be one boundary pixel that presents the least capillary resistance (largest percolating pore radius) and the injected fluid will traverse this least resistant pixel. Since there is quenched disorder in the material, the spatial location of this least-resistant boundary pixel at any instant will be random so that a fractal structure tends to develop (this corresponds to the invasion percolation model). As rates increase, multiple boundary pixels must simultaneously be invaded in order to accommodate the injected fluid and this is possible because many boundary pixels now exceed the capillary-resistance threshhold due to the elevated injection pressure. Thus, as injection rates increase, a more regular distribution of boundary pixels surrounding the injection point will be invaded and this leads to a more ball-like structure.

The point for our work here is that at any instant it is the boundary pixels that are always able to provide the least capillary resistance. The interior pixels have already been traversed and thus contain meniscii that are necessarily trapped on more resistive parts of the pore space. This image of the invasion process works for either drainage or imbibition but will ultimately break down at sufficiently high-injection rates.

III. TWO-PHASE FLOW AT THE PORE SCALE

With the above ideas in mind, we now lay out the boundary-value problem controlling the flow in each averaging volume (or interior pixel). The region Ω occupied by an averaging volume is partitioned into three parts $\Omega = \Omega_a + \Omega_b + \Omega_g$ corresponding to fluid a, fluid b, and the solid grains g. The surfaces $\partial\Omega_f$ ($f = a$ or b) enclosing the fluid regions Ω_f also consist of three parts,

$$\partial\Omega_f = \partial E_f + \partial G_f + \partial F, \tag{20}$$

where ∂E_f is the surface coincident with the external surface of the averaging volume (the entrance and exit surfaces), ∂G_f is the surface coincident with the grain surfaces, and ∂F is the fluid interface (the meniscii).

The equations governing the two-phase flow are

$$\nabla \cdot \mathbf{T}_f + \rho_f \mathbf{g} = \rho_f \partial \mathbf{v}_f / \partial t \quad \text{in } \Omega_f, \tag{21}$$

$$\mathbf{T}_f = -P_f \mathbf{I} + \eta_f [\nabla \mathbf{v}_f + (\nabla \mathbf{v}_f)^T] \quad \text{in } \Omega_f, \tag{22}$$

$$\nabla \cdot \mathbf{v}_f = 0 \quad \text{in } \Omega_f, \tag{23}$$

$$[\mathbf{v}_f] = 0; \quad \mathbf{n} \cdot \mathbf{v}_a = v_\zeta; \quad \mathbf{n} \cdot [\mathbf{T}_f] = \sigma H \mathbf{n} \text{ on } \partial F, \tag{24}$$

where $\mathbf{T}_f$ is the total stress tensor in the fluid, P_f is the total pressure, η_f is the viscosity, v_ζ is the rate at which the interface ∂F is displacing, H is the interface curvature (as defined in Appendix A), σ is the surface tension, and the brackets [ ] indicate the change in a field as the interface is traversed from a toward b (which is the sense of the interface normal $\mathbf{n}$). In addition to these boundary conditions on ∂F, the no-slip flow condition $\mathbf{v}_f = \mathbf{0}$ holds on all grain surfaces ∂G_f.

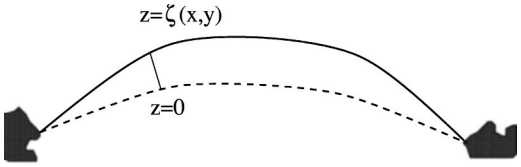

FIG. 3. The surface $z = \zeta(x,y)$ represents the position of the fluid interface at any instant while the initial interface position is denoted by $z = 0$. The curvilinear coordinates x and y denote positions along the initial interface.

As stated, we consider an initial state of no flow in which gravity alone produces the static pressure distributions $P_f^o(\mathbf{r}) = \mathcal{P}_f - \rho_f \mathbf{g} \cdot \mathbf{r}$. This allows the total pressure to be written

$$P_f(\mathbf{r},t) = P_f^o(\mathbf{r}) + \overline{p}_f(t) - \mathbf{F}_f(t) \cdot \mathbf{r} + \pi_f(\mathbf{r},t), \tag{25}$$

where $\mathbf{F}_f(t)$ are the uniform-force densities and $\overline{p}_f(t)$ are the uniform pressures applied to each averaging volume by some distant injection process as discussed in the previous section.

The main role of the static state in the present argument is to fix an initial position of the fluid interface. For the argument, we assume this interface position is known. Once $\overline{p}_f(t)$ and $\mathbf{F}_f(t)$ are applied, the theory is to supply rules for how the interface will displace as well as give a complete solution to the flow problem.

As shown in Fig. 3, we denote the normal displacement of the interface from its initial position as ζ. In Appendix A, we work in the (x,y,z) curvilinear coordinates shown in the figure to obtain an exact expression for the nonlinear differential operator $H(\zeta)$. For now, we simply write

$$H(\zeta) = H_o + h(\zeta), \tag{26}$$

where H_o is the initial curvature (related to the static pressures as $\sigma H_o = P_c^o$) while the operator $h(\zeta)$ gives the change in curvature due to the applied forces. The rate of displacement function v_ζ is given by

$$v_\zeta = \mathbf{n} \cdot \hat{\mathbf{z}} \partial\zeta / \partial t. \tag{27}$$

As seen in the Appendix, when displacement cannot be considered small, the operator $h(\zeta)$ is extremely nonlinear as are the expressions for the interface normal $\mathbf{n}$ and tangent vectors $\mathbf{t}_x$ and $\mathbf{t}_y$. Thus, because ζ is one of the unknowns, this two-phase flow problem can be highly nonlinear due to the boundary conditions on ∂F.

Such nonlinearity means that the response due to $\overline{p}_f$ cannot be resolved from that due to $\mathbf{F}_f$. However, it will be shown that for given values of the $\overline{p}_f$, the viscous flow produced by $\mathbf{F}_f$ only weakly perturbs the interface in comparison to the possibly large displacements produced by $\overline{p}_f$. Thus, the result of the perturbation analysis of the following section is that the interface displacement and flow fields can be solved in two steps: (i) apply the $\overline{p}_f$ while keeping $\mathbf{F}_f$

$=\mathbf{0}$ and determine a new interface position, then (ii) add on the $\mathbf{F}_f$ to determine the flow fields and additional (small) interface displacements.

To obtain this procedure, the dimensions must first be removed. We allow $\mathbf{F}_a(t)$ and $\mathbf{F}_b(t)$ to have different amplitudes and direction, and to vary over time scales t_F that are slow enough that inertial effects (such as capillary waves and viscous boundary layers) remain negligible. These forces have a characteristic value $\mathcal{F}$ that can be related to the pressure $\Delta\mathcal{P}$ applied at an injection/extraction point as

$$\mathcal{F}=\Delta\mathcal{P}/\mathcal{L}, \tag{28}$$

where $\mathcal{L}$ is a macroscopic length such as the distance between an injection point and the distant invasion front. We take $\Delta\mathcal{P}$ as a characteristic measure of the $\overline{p_f}$. Last, we define a characteristic pore size ℓ_c.

With these identifications, the dimensions are now removed using the following definitions in which primed fields have their dimensions while unprimed fields do not:

$$\begin{gathered}\mathbf{F}_f=\mathcal{F}\mathbf{F}_f', \quad \overline{p_f}=\Delta\mathcal{P}\overline{p_f'}, \\ \mathbf{v}_f=\frac{\eta_a}{\mathcal{F}\ell_c^2}\mathbf{v}_f', \quad \pi_f=\frac{1}{\mathcal{F}\ell_c}\pi_f', \\ H=\ell_c H', \quad \zeta=\zeta'/\ell_c, \\ \nabla=\ell_c\nabla', \quad t=t'/t_F.\end{gathered} \tag{29}$$

Thus, the dimensionless-flow problem is defined as

$$\nabla\cdot\boldsymbol{\tau}_f+\mathbf{F}_f=\mathbf{0} \quad \text{in } \Omega_f, \tag{30}$$

$$\nabla\cdot\mathbf{v}_f=\mathbf{0} \quad \text{in } \Omega_f, \tag{31}$$

$$\boldsymbol{\tau}_a=-\pi_a\mathbf{I}+\nabla\mathbf{v}_a+(\nabla\mathbf{v}_a)^T \quad \text{in } \Omega_a, \tag{32}$$

$$\boldsymbol{\tau}_b=-\pi_b\mathbf{I}+\gamma[\nabla\mathbf{v}_b+(\nabla\mathbf{v}_b)^T] \quad \text{in } \Omega_b, \tag{33}$$

$$[\mathbf{v}_f]=0 \quad \text{on } z=\zeta, \tag{34}$$

$$\mathbf{n}\cdot\mathbf{v}_a=\chi\mathbf{n}\cdot\hat{\mathbf{z}}\frac{\partial\zeta}{\partial t} \quad \text{on } z=\zeta, \tag{35}$$

$$\mathbf{n}\cdot[\boldsymbol{\tau}_f]\cdot\mathbf{t}=\mathbf{0} \quad \text{on } z=\zeta, \tag{36}$$

$$\epsilon\{\mathbf{n}\cdot[\boldsymbol{\tau}_f]\cdot\mathbf{n}+(\mathbf{F}_b-\mathbf{F}_a)\cdot\mathbf{r}\}+\frac{\epsilon}{\alpha}(\overline{p_a}-\overline{p_b})=h(\zeta) \quad \text{on } z=\zeta, \tag{37}$$

and is completed by taking $\pi_f=0$ on the external faces of the averaging volume.

Four dimensionless numbers appear,

$$\epsilon=\frac{\mathcal{F}\ell_c^2}{\sigma}, \quad \gamma=\frac{\eta_b}{\eta_a}, \quad \chi=\frac{\eta_a}{t_F\mathcal{F}\ell_c}, \quad \alpha=\frac{\ell_c}{\mathcal{L}}. \tag{38}$$

The capillary number ϵ controls the degree to which the interface is displaced by viscous forcing (as $\epsilon\to 0$ the viscous forces are incapable of moving the interface), the viscosity ratio γ controls the amount of viscous coupling across the interface (as $\gamma\to 0$ such cross-coupling becomes negligible), while the rate number χ is the ratio between the time a fluid particle spends in a pore and the applied-force variation time t_F (as $\chi\to 0$, one can assume the flow is always in the steady state).

In the following section we perform a perturbation analysis using ϵ as the small parameter. It is thus important to establish careful estimates of the size of the other dimensionless numbers in comparison to ϵ. To do so, we first assume a maximum applied pressure consistent with the fixed contact-line condition of Eq. (3),

$$\Delta\mathcal{P}\lesssim\sigma/\ell_c. \tag{39}$$

Next, since the time variation of the macroscopic pressure is due to diffusion, we propose a characteristic relation between t_F and $\mathcal{L}$ of the form

$$t_F=\mathcal{L}^2/D=\eta_a\beta_a\mathcal{L}^2/k, \tag{40}$$

where D is the two-phase-flow pressure diffusivity of the porous material. Here, we have assumed fluid a to be the invading fluid and determined D using our final laws. We have that $D=k/(\eta_a\beta_a)$, where η_a is the viscosity of fluid a, k is the permeability [we do not multiply by the $O(1)$ relative permeability in this order-of-magnitude estimate], and $\beta_a=\partial\varphi_a/\partial P_c$ and controls how saturation changes when capillary pressure changes.

Upon introducing these estimates into Eq. (38), we obtain

$$\alpha=\frac{\ell_c}{\mathcal{L}}\gtrsim\epsilon \quad \text{and} \quad \chi\gtrsim\frac{k}{\sigma\beta_a\mathcal{L}}. \tag{41}$$

For applied forces that do not migrate contact lines behind the invasion front (the regime of this paper), we see that ϵ can be an extremely small number. Assuming the following characteristic values $\sigma\sim 10^{-3}$ Pa m, $\beta_a\sim 10^{-5}$ Pa^{-1}, and $k\sim 10^{-11}$ m^2 (high permeability), we find that $k/(\sigma\beta_a)=10^{-3}$ m. Thus, for diffusion through high-permeability laboratory samples $\mathcal{L}\sim 10^{-1}$ m, we have $\chi\gtrsim 10^{-2}$, which can be considered $O(1)$ relative to ϵ. However, the situation of practical interest is when rocks are experiencing diffusion over distances in the earth. For such problems, we easily enter the regime where $\chi=O(\epsilon)$, as will be discussed in detail in the final section.

We will perform the analysis here assuming $\chi=O(1)$. The modifications of the final laws for the case where $\chi=O(\epsilon)$ will be obvious since all the χ dependence will appear explicitly. Last, the viscosity ratio γ will also be taken as $O(1)$.

IV. ASYMPTOTIC SOLUTION OF THE PORE-SCALE PROBLEM

In order to arrive at the perturbation scheme in an efficient manner, let us begin by defining, somewhat out of the blue, the leading-order problem in ϵ when $P_c=\overline{p_a}-\overline{p_b}$ acts alone; i.e., set $\mathbf{F}_f=\mathbf{0}$ in Eqs. (30)–(37) and ignore any term multiplied by ϵ. This capillary-pressure problem is defined as

$$\nabla\cdot\boldsymbol{\tau}_{f0}^P=\mathbf{0} \quad \text{in } \Omega_{fo}, \tag{42}$$

$$[\mathbf{v}_{f0}^P]=0 \quad \text{on } z=\zeta_o, \tag{43}$$

$$\mathbf{n}_o\cdot\mathbf{v}_{a0}^P=\chi\mathbf{n}_o\cdot\hat{\mathbf{z}}\frac{\partial\zeta_o}{\partial t} \quad \text{on } z=\zeta_o, \tag{44}$$

$$\mathbf{n}_o\cdot[\boldsymbol{\tau}_{f0}^P]\cdot\mathbf{t}_o=\mathbf{0} \quad \text{on } z=\zeta_o, \tag{45}$$

$$P_c(t)\equiv\overline{p_a}-\overline{p_b}=h(\zeta_o) \quad \text{on } z=\zeta_o, \tag{46}$$

where the superscript P indicates that these fields are due to capillary pressure alone while the subscript 0 indicates that they are leading order in ϵ. The reason for such a notation will be seen shortly. Although we cease to write out $\nabla\cdot\mathbf{v}=\mathbf{0}$ and the constitutive laws for $\boldsymbol{\tau}$, they are to be understood as part of the problem statement.

The key property of these equations is that the differential equation $h(\zeta_o)=P_c(t)$ in the boundary condition (46), along with the condition that $\zeta_o=0$ on all contact lines, is sufficient to determine the displacement function

$$\zeta_o=\zeta_o(x,y;P_c(t)) \tag{47}$$

which has, in general, a highly nonlinear dependence on P_c. Given this function, the normal $\mathbf{n}_o$ and tangent vectors $\mathbf{t}_o$ of $z=\zeta_o$ can be determined which permits the flow field excited by the interface displacement of Eq. (44) to be uniquely determined and expressed in the form

$$\mathbf{v}_{f0}^P(\mathbf{r},t)=\left[\int\frac{dxdy}{h_xh_y}\hat{\mathbf{z}}\cdot\mathbf{M}(\mathbf{r}|x,y;P_c)\frac{\partial\zeta_o(x,y;P_c)}{\partial P_c}\right]\chi\frac{\partial P_c}{\partial t}. \tag{48}$$

This solution is linear in $\partial P_c/\partial t$ but extremely nonlinear in P_c. Upon averaging over the volume Ω_{fo} (i.e., the region of fluid f in an averaging volume when the interface is at $z=\zeta_o$), we have

$$\langle\mathbf{v}_{f0}^P\rangle=\chi\mathbf{m}_f\frac{\partial P_c}{\partial t}, \tag{49}$$

where the transport coefficient $\mathbf{m}_f$ is thus defined as

$$\mathbf{m}_f=\frac{1}{V}\int_{\Omega_{fo}}d^3\mathbf{r}\int\frac{dx\,dy}{h_xh_y}\hat{\mathbf{z}}\cdot\mathbf{M}_f(\mathbf{r}|x,y;P_c)\frac{\partial\zeta_o(x,y;P_c)}{\partial P_c}.$$

We will discuss the meaning of the $\mathbf{m}_f$ later (they only exist in the presence of a saturation gradient). An important property of this flow, if it exists, is that it ceases once the capillary pressure ceases to change.

Given these initial results, we now treat the complete flow problem by means of a perturbation analysis using the capillary number ϵ as the small parameter. In order to properly affectuate the analysis, it is convenient to first define new surface coordinates (x_o,y_o,z_o) attached to the capillary-pressure surface $z=\zeta_o$ determined by Eq. (47) and as shown in Fig. 4. In these new coordinates, the surface $z_o=0$ corresponds to $z=\zeta_o$ in the old coordinates and so $\hat{\mathbf{z}}_o=\mathbf{n}_o$, $\hat{\mathbf{x}}_o=\mathbf{t}_{xo}$, and $\hat{\mathbf{y}}_o=\mathbf{t}_{yo}$.

We start afresh and restate the entire dimensionless-flow problem using (x_o,y_o,z_o),

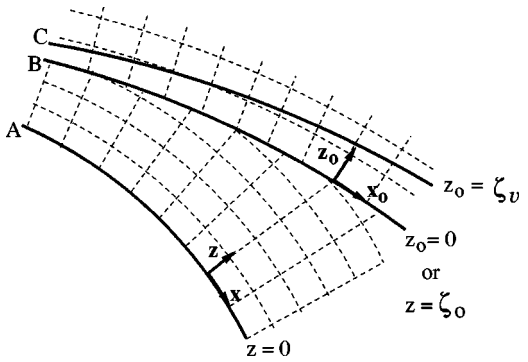

FIG. 4. The two sets of surface coordinates and the fluid interface in three positions: curve *A*, the initial static-state position $z=0$; curve *B*, the position when $P_c=\overline{p_a}-\overline{p_b}$ acts alone and defined $z=\zeta_0$ in the initial coordinates or $z_o=0$ in the new coordinates (x_o,y_o,z_o); and curve *C*, the actual position when P_c and $\mathbf{F}_f$ both act.

$$\nabla\cdot\boldsymbol{\tau}_f+\mathbf{F}_f=\mathbf{0} \quad \text{in } \Omega_f, \tag{50}$$

$$[\mathbf{v}_f]=0 \quad \text{on } z_o=\zeta_v, \tag{51}$$

$$\mathbf{n}\cdot\mathbf{v}_a=\chi\mathbf{n}\cdot\left(\hat{\mathbf{z}}\frac{\partial\zeta_o}{\partial t}+\hat{\mathbf{z}}_o\frac{\partial\zeta_v}{\partial t}\right) \quad \text{on } z_o=\zeta_v, \tag{52}$$

$$\mathbf{n}\cdot[\boldsymbol{\tau}_f]\cdot\mathbf{t}=\mathbf{0} \quad \text{on } z_o=\zeta_v, \tag{53}$$

$$\epsilon\{\mathbf{n}\cdot[\boldsymbol{\tau}_f]\cdot\mathbf{n}+(\mathbf{F}_b-\mathbf{F}_a)\cdot\mathbf{r}\}+P_c=H(\zeta_v) \quad \text{on } z_o=\zeta_v. \tag{54}$$

The surface $z_o=\zeta_v$ is the final unknown position of the fluid interface. The subscript v indicates that this part of the displacement is due to viscous flow. The known displacement vector $\hat{\mathbf{z}}\zeta_o$ is now to be understood as a function of (x_o,y_o).

To obtain asymptotically correct results through all orders of ϵ, we must first continue the boundary conditions from the unknown surface $z_o=\zeta_v$ to the known surface $z_o=0$ by means of a Taylor-series development around $z_o=0$,

$$[\mathbf{v}_f]+\left[\frac{\partial\mathbf{v}_f}{\partial z_o}\right]\zeta_v+\cdots=0, \tag{55}$$

$$\mathbf{n}\cdot\left(\mathbf{v}_a+\frac{\partial\mathbf{v}_a}{\partial z_o}\zeta_v+\cdots\right)=\chi\mathbf{n}\cdot\left(\hat{\mathbf{z}}\frac{\partial\zeta_o}{\partial t}+\hat{\mathbf{z}}_o\frac{\partial\zeta_v}{\partial t}\right), \tag{56}$$

$$\mathbf{n}\cdot\left([\boldsymbol{\tau}_f]+\left[\frac{\partial\boldsymbol{\tau}_f}{\partial z_o}\right]\zeta_v+\cdots\right)\cdot\mathbf{t}=0, \tag{57}$$

$$\epsilon\mathbf{n}\cdot\left([\boldsymbol{\tau}_f]+\left[\frac{\partial\boldsymbol{\tau}_f}{\partial z_o}\right]\zeta_v+\cdots\right)\cdot\mathbf{n}+\epsilon(\mathbf{F}_b-\mathbf{F}_a)\cdot\mathbf{r}+P_c=H(\zeta_v). \tag{58}$$

All flow fields in these boundary conditions are now being evaluated at (or across) $z_o=0$. Due to the smoothness of the low-Reynold's-number flow, such expansions can be considered uniformly valid.

We can at last perform the perturbation expansions by means of the asymptotic series

$$\mathbf{v}_f=\mathbf{v}_{f0}+\epsilon\mathbf{v}_{f1}+O(\epsilon^2), \tag{59}$$

$$\boldsymbol{\tau}_f = \boldsymbol{\tau}_{f0} + \epsilon \boldsymbol{\tau}_{f1} + O(\epsilon^2), \tag{60}$$

$$\zeta_v = \epsilon \zeta_1 + O(\epsilon^2). \tag{61}$$

There is no zeroth-order term for ζ_v because this displacement is produced entirely by viscous forces. We also have the following results from Appendix A concerning the surface properties of $z_o = \zeta_v$,

$$\mathbf{n} = \hat{\mathbf{z}}_o - \epsilon \nabla \zeta_1 + O(\epsilon^2), \tag{62}$$

$$\mathbf{t}_x = \hat{\mathbf{x}}_o + \epsilon h_{xo} \frac{\partial \zeta_1}{\partial x_o} \hat{\mathbf{z}}_o + O(\epsilon^2), \tag{63}$$

$$\mathbf{t}_y = \hat{\mathbf{y}}_o + \epsilon h_{yo} \frac{\partial \zeta_1}{\partial y_o} \hat{\mathbf{z}}_o + O(\epsilon^2), \tag{64}$$

$$H(\zeta_v) = H(0) - \epsilon [\nabla^2 \zeta_1 + \xi^2 \zeta_1] + O(\epsilon^2), \tag{65}$$

where $H(0)$ is the known curvature of the capillary-pressure surface $z_o = 0$. When all of this is inserted into the governing equations, we obtain a hierarchy of linear subproblems in powers of ϵ each defined in the same known domains Ω_{fo} and with boundary conditions on the same known surface $z_o = 0$.

The ϵ^0 flow fields separate into two contributions $\mathbf{v}_{f0} = \mathbf{v}_{f0}^P + \mathbf{v}_{f0}^F$ which derive, respectively, from (i) the capillary-pressure problem of Eqs. (42)–(46) that has already been treated; and (ii) the Stokes-flow problem given by

$$\nabla \cdot \boldsymbol{\tau}_{f0}^F + \mathbf{F}_f = \mathbf{0} \quad \text{in } \Omega_{fo}, \tag{66}$$

$$[\mathbf{v}_{f0}^F] = \mathbf{0}; \quad \text{on } z_o = 0, \tag{67}$$

$$\hat{\mathbf{z}}_o \cdot \mathbf{v}_{a0}^F = \mathbf{0} \quad \text{on } z_o = 0, \tag{68}$$

$$\hat{\mathbf{z}}_o \cdot [\boldsymbol{\tau}_{f0}^F] \cdot (\hat{\mathbf{x}}_o \text{ and } \hat{\mathbf{y}}_o) = \mathbf{0} \quad \text{on } z_o = 0. \tag{69}$$

The unique solution for $\mathbf{v}_{f0}^F$ can be expressed as

$$\mathbf{v}_{f0}^F(\mathbf{r},t) = \sum_{f'=a}^{b} \mathbf{N}_{ff'}(\mathbf{r};P_c) \cdot \mathbf{F}_{f'}(t), \tag{70}$$

where the four response tensors $\mathbf{N}_{ff'}(\mathbf{r};P_c)$ are all highly nonlinear functions of P_c. Upon averaging this flow over the domain of Ω_{fo}, we obtain the macroscopic laws

$$\langle \mathbf{v}_{f0}^F \rangle = \sum_{f'=a}^{b} \mathbf{L}_{ff'} \cdot \mathbf{F}_{f'}, \tag{71}$$

where the transport tensors are defined as

$$\mathbf{L}_{ff'} = \frac{1}{V} \int_{\Omega_{fo}} d^3\mathbf{r} \mathbf{N}_{ff'}(\mathbf{r};P_c). \tag{72}$$

The symmetry properties of these transport tensors will be addressed in a later section.

The normal-stress boundary condition involving the ϵ^0 fields is

$$\nabla^2 \zeta_1 + \xi^2 \zeta_1 = -\hat{\mathbf{z}}_o \cdot [\boldsymbol{\tau}_{f0}] \cdot \hat{\mathbf{z}}_o + (\mathbf{F}_a - \mathbf{F}_b) \cdot \mathbf{r}, \tag{73}$$

where the source term $\hat{\mathbf{z}}_o \cdot [\boldsymbol{\tau}_{f0}] \cdot \hat{\mathbf{z}}_o$ has contributions from both the capillary-pressure flow $\mathbf{v}_{f0}^P$ and the Stokes flow $\mathbf{v}_{f0}^F$. Along with the no-slip condition at the contact lines, this linear differential equation allows the first correction of the interface displacement due to viscous flow to be expressed in the separated form $\zeta_1 = \zeta_1^F + \zeta_1^P$, where

$$\hat{\mathbf{z}}_o \zeta_1^F(x_o, y_o, t) = \sum_{f=a}^{b} \mathbf{Z}_f(x_o, y_o; P_c) \cdot \mathbf{F}_f, \tag{74}$$

$$\zeta_1^P(x_o, y_o, t) = \chi \mathcal{Z}(x_o, y_o; P_c) \partial P_c / \partial t, \tag{75}$$

and where the response tensor $\mathbf{Z}_f(x_o, y_o; P_c)$ and scalar $\mathcal{Z}(x_o, y_o; P_c)$ are, as well, nonlinear functions of P_c.

The ϵ^1 problem is now stated (and after this we stop)

$$\nabla \cdot \boldsymbol{\tau}_{f1} = \mathbf{0} \quad \text{in } \Omega_{fo}, \tag{76}$$

$$[\mathbf{v}_{f1}] = -\zeta_1 \left[\frac{\partial \mathbf{v}_{f0}}{\partial z_o} \right] \quad \text{on } z_o = 0, \tag{77}$$

$$\hat{\mathbf{z}}_o \cdot \mathbf{v}_{a1} = \nabla \zeta_1 \cdot \mathbf{v}_{a0} - \zeta_1 \hat{\mathbf{z}}_o \cdot \frac{\partial \mathbf{v}_{a0}}{\partial z_o} + \chi \left(\frac{\partial \zeta_1}{\partial t} - \hat{\mathbf{z}}_o \cdot \nabla \zeta_1 \frac{\partial \zeta_o}{\partial t} \right) \quad \text{on } z_o = 0, \tag{78}$$

$$\hat{\mathbf{z}}_o \cdot [\boldsymbol{\tau}_{f1}] \cdot \hat{\mathbf{x}}_o = \nabla \zeta_1 \cdot [\boldsymbol{\tau}_{f0}] \cdot \hat{\mathbf{x}}_o - h_{xo} \frac{\partial \zeta_1}{\partial x_o} \hat{\mathbf{z}}_o \cdot [\boldsymbol{\tau}_{f0}] \cdot \hat{\mathbf{z}}_o - \zeta_1 \hat{\mathbf{z}}_o \cdot \left[\frac{\partial \boldsymbol{\tau}_{f0}}{\partial z_o} \right] \cdot \hat{\mathbf{x}}_o \quad \text{on } z_o = 0, \tag{79}$$

where only the x_o component of the shear traction boundary condition has been given but there is an analogous y_o component as well.

This problem is completely linear in the first-order fields. All terms on the right-hand side of the boundary conditions are known and act as flow-inducing forces. Due to the linearity, the response from each such inhomogeneous boundary term can be determined independently (i.e., with the other inhomogeneous terms set to zero) and the results summed to give the total response. Due to the separations $\zeta_1 = \zeta_1^P + \zeta_1^F$ and $\mathbf{v}_0 = \mathbf{v}_0^P + \mathbf{v}_0^F$ already treated, each term in the boundary conditions is seen to be proportional to one of the five following macroscopic-forcing forms: (a) $\mathbf{F}_f \mathbf{F}_{f'}$, (b) $\chi \partial \mathbf{F}_f / \partial t$, (c) $\chi \mathbf{F}_f \partial P_c / \partial t$, (d) $\chi^2 \partial P_c / \partial t$, and (e) $\chi^2 (\partial P_c / \partial t)^2$. For example, the boundary term $\chi \partial \zeta_1^P / \partial t$ in Eq. (78) gives rise to both forms (d) and (e). Thus, the macroscopic transport associated with the ϵ^1 problem can be expressed as

$$\langle \mathbf{v}_{f1} \rangle = \sum_{f'=a}^{b} \sum_{f''=a}^{b} {}_3\mathbf{A}_{ff'f''}(P_c) : \mathbf{F}_{f'}\mathbf{F}_{f''} + \chi \sum_{f'=a}^{b} \mathbf{B}_{ff'}(P_c) \cdot \partial \mathbf{F}_{f'}/\partial t + \chi \sum_{f'=a}^{b} \mathbf{C}_{ff'}(P_c) \cdot \mathbf{F}_{f'} \partial P_c/\partial t + \chi^2 [\mathbf{d}_f(P_c) + \mathbf{e}_f(P_c) \partial P_c/\partial t] \partial P_c/\partial t, \tag{80}$$

where the eight transport triads (third-order tensors) ${}_3\mathbf{A}_{ff'f''}$, the eight transport dyads $\mathbf{B}_{ff'}$ and $\mathbf{C}_{ff'}$, and the four transport vectors $\mathbf{d}_f$ and $\mathbf{e}_f$ are all nonlinear functions of P_c. An enormous number of transport coefficients have entered this ϵ^1 contribution and the situation becomes exponentially worse as higher-order contributions are considered.

Before we treat the symmetry properties of these laws and summarize them, we first establish the macroscopic fluid-conservation laws and consider the connection between $\langle \mathbf{v}_f \rangle$ and what is actually measured during flow experiments.

V. FLUID CONSERVATION

Both Whitaker [8] and Auriault [9] have addressed the fluid-conservation laws using volume-averaging arguments, so just a brief outline is given here.

The definition of the derivative of a volume-averaged quantity is again used to write

$$\nabla \cdot \langle \mathbf{v}_f \rangle = \frac{1}{V} \int_{\partial E_f} \mathbf{n} \cdot \mathbf{v}_f dS. \tag{81}$$

The incompressibility condition $\nabla \cdot \mathbf{v}_f = \mathbf{0}$ is then averaged and the divergence theorem applied to obtain

$$0 = \frac{1}{V} \int_{\partial E_f} \mathbf{n} \cdot \mathbf{v}_f dS + \frac{1}{V} \int_{\partial F} \mathbf{n}_f \cdot \mathbf{v}_a dS, \tag{82}$$

where on ∂F we have $\mathbf{n}_a = +\mathbf{n}$ while $\mathbf{n}_b = -\mathbf{n}$. The integral over ∂F can be identified as the time rate of change of the fluid-a volume fraction,

$$\frac{\partial \varphi_a}{\partial t} \equiv \frac{1}{V} \int_{\partial F} \mathbf{n} \cdot \mathbf{v}_a dS, \tag{83}$$

so that the fluid-conservation laws take the form

$$\nabla \cdot \langle \mathbf{v}_a \rangle = -\frac{\partial \varphi_a}{\partial t}, \tag{84}$$

$$\nabla \cdot \langle \mathbf{v}_b \rangle = +\frac{\partial \varphi_a}{\partial t}. \tag{85}$$

For incompressible two-phase flow, the total fluid flux is conserved $\nabla \cdot [\langle \mathbf{v}_a \rangle + \langle \mathbf{v}_b \rangle] = 0$.

We can use the boundary condition (52) in the above definition of $\partial \varphi_a/\partial t$ to establish through $O(\epsilon)$

$$\frac{\partial \varphi_a}{\partial t} = \frac{\chi}{V} \int \frac{dx_o dy_o}{h_{xo} h_{yo}} \left\{ \hat{\mathbf{z}}_o \cdot \hat{\mathbf{z}} \frac{\partial \zeta_o}{\partial t} + \epsilon \left[\frac{\partial \zeta_1}{\partial t} - \nabla \zeta_1 \cdot \hat{\mathbf{z}} \frac{\partial \zeta_o}{\partial t} \right] \right\}. \tag{86}$$

Due to the known force dependences of ζ_o and ζ_1, we can immediately write the forms

$$\frac{\partial \varphi_a}{\partial t} = \chi \mathcal{S}_0(P_c) \frac{\partial P_c}{\partial t} + \epsilon \chi^2 \mathcal{S}_1(P_c) \left(\frac{\partial P_c}{\partial t} \right)^2 + \epsilon \chi \sum_{f=a}^{b} \left[\mathbf{s}_f(P_c) \cdot \frac{\partial \mathbf{F}_f}{\partial t} + \mathbf{t}_f(P_c) \cdot \mathbf{F}_f \frac{\partial P_c}{\partial t} \right]. \tag{87}$$

The various coefficients $\mathcal{S}_0$, $\mathcal{S}_1$, $\mathbf{s}_f$, and $\mathbf{t}_f$ are nonlinear functions of P_c. Both $\mathcal{S}_0$ and $\mathbf{s}_f$ can be readily measured in a laboratory; however, the measurement of $\mathbf{t}_f$ and $\mathcal{S}_1$ is likely to be much more subtle. We underline that any such measurements must be performed on samples containing percolating fluids when both $P_c = 0$ and $\mathbf{F}_f = \mathbf{0}$. This expression for $\partial \varphi_a/\partial t$ is what closes the system of macroscopic equations.

VI. FLUID FLUX

The issue addressed here is the connection between the volume-averaged flow $\langle \mathbf{v}_f \rangle$ and the flux $\mathbf{J}_f$ that is actually measured during experiments. Auriault [9] considered this connection only for steady-state situations in which the interface is not moving. We discuss here the more general situation in which saturation levels are changing in a sample.

The relation between a volume average and a flux is obtained by volume integrating the identity $\nabla \cdot (\mathbf{v}_f \mathbf{r}) = \mathbf{r}(\nabla \cdot \mathbf{v}_f) + \mathbf{v}_f \cdot \nabla \mathbf{r} = \mathbf{v}_f$ to give [13]

$$\langle \mathbf{v}_f \rangle = \frac{1}{V} \int_{\partial E_f} \mathbf{n} \cdot \mathbf{v}_f \mathbf{r} dS + \frac{1}{V} \int_{\partial F} \mathbf{n}_f \cdot \mathbf{v}_a \mathbf{r} dS. \tag{88}$$

Note that from Eq. (82), this definition of $\langle \mathbf{v}_f \rangle$ is independent of the origin of $\mathbf{r}$. However, the physical interpretation of the two surface integrals is affected by the choice of origin. In what follows, we assume $\mathbf{r}$ has its origin at the center of the averaging volume.

Appealing to any specific averaging volume (such as the disk considered earlier) demonstrates that

$$\mathbf{J}_f \equiv \frac{1}{V} \int_{\partial E_f} \mathbf{n} \cdot \mathbf{v}_f \mathbf{r} dS \tag{89}$$

is the average rate at which fluid f is fluxing across all exterior surfaces ∂E of a sample. The flux $\mathbf{J}_f$, as defined by Eq. (89), is something that can be experimentally observed and measured in the laboratory. The other contribution to $\langle \mathbf{v}_f \rangle$ has an interpretation analogous to Eq. (83),

$$\frac{\partial \mathbf{r}_a}{\partial t} \equiv \frac{1}{V} \int_{\partial F} \mathbf{n} \cdot \mathbf{v}_a \mathbf{r} dS, \tag{90}$$

where the point $\mathbf{r}_a$ is a measure of the center of the fluid-a distribution in an averaging volume and is defined as

$$\mathbf{r}_a \equiv \frac{1}{V} \int_{\Omega_a} \mathbf{r} dV. \tag{91}$$

We will consider how $\partial \mathbf{r}_a/\partial t$ can be experimentally measured momentarily.

The relations we seek are thus of the form

$$\langle \mathbf{v}_a \rangle = \mathbf{J}_a + \frac{\partial \mathbf{r}_a}{\partial t}, \tag{92}$$

$$\langle \mathbf{v}_b \rangle = \mathbf{J}_b - \frac{\partial \mathbf{r}_a}{\partial t}. \tag{93}$$

Since $\partial \mathbf{r}_a/\partial t$ represents the moment of the saturation changes across a sample, the volume-averaged flow can be taken as the measured flux only if the local saturation is changing rather uniformly across a sample or if the interface is in a steady state. We underline that the average flow $\langle \mathbf{v}_f \rangle$ cannot be directly measured in the laboratory. What is normally measured is the flux across entrance and exit surfaces of a sample, which is equivalent to measuring $\mathbf{J}_f$ (the average flux over both the entrance and the exit surfaces) and $\partial \varphi_a/\partial t$ (the difference between the entrance and exit fluxes).

Because of the form of the conservation laws (84) and (85), we want to express the transport laws of the theory in terms of $\langle \mathbf{v}_f \rangle$. However, for all of the coefficients in such transport laws to be measurable in the laboratory, Eqs. (92) and (93) show that we must have a way to measure $\partial \mathbf{r}_a/\partial t$. If the fluid densities are different ($\rho_a \neq \rho_b$), the following is one such measurement procedure.

The center of mass $\mathbf{r}_{\rm cm}$ of the fluid-filled pore space is defined as

$$\mathbf{r}_{\rm cm} = \frac{\int_{\Omega_a} \rho_a \mathbf{r} dV + \int_{\Omega_b} \rho_b \mathbf{r} dV}{V\varphi_a\rho_a + V\varphi_b\rho_b} \tag{94}$$

$$= \frac{\rho_a \mathbf{r}_a + \rho_b \mathbf{r}_b}{\varphi_a\rho_a + \varphi_b\rho_b}. \tag{95}$$

We write $\varphi_b(t) = \phi - \varphi_a(t)$, where ϕ is the constant porosity in a sample, multiply both sides of Eq. (95) by $\varphi_a\rho_a + \varphi_b\rho_b$, and then take the time derivative to obtain

$$\frac{\partial \mathbf{r}_a}{\partial t} = \mathbf{r}_{\rm cm}\frac{\partial \varphi_a}{\partial t} + \left(\frac{\phi\rho_b}{\rho_a - \rho_b} + \varphi_a \right) \frac{\partial \mathbf{r}_{\rm cm}}{\partial t}. \tag{96}$$

We have used the fact that $\partial \mathbf{r}_b/\partial t = -\partial \mathbf{r}_a/\partial t$. Thus, the measurement of $\partial \mathbf{r}_a/\partial t$ has been reduced to measuring the changes in the center of mass of the pore space. Since the grains do not redistribute, this can be performed by placing a horizontal sample on a support that is sensitive to the sample's weight at various points along its length.

VII. SYMMETRY OF THE TRANSPORT LAWS

We now write out the transport laws obtained earlier,

$$\begin{aligned}\langle \mathbf{v}_a \rangle = {} & \mathbf{L}_{aa}\cdot\mathbf{F}_a + \mathbf{L}_{ab}\cdot\mathbf{F}_b + \chi\mathbf{m}_a\frac{\partial P_c}{\partial t} \\ & + \epsilon\sum_{f=a}^{b}\sum_{f'=a}^{b} {}_3\mathbf{A}_{aff'}:\mathbf{F}_{f'}\mathbf{F}_f + \epsilon\chi\sum_{f=a}^{b}\left[\mathbf{B}_{af}\cdot\frac{\partial \mathbf{F}_f}{\partial t}\right. \\ & \left. + \mathbf{C}_{af}\cdot\mathbf{F}_f\frac{\partial P_c}{\partial t}\right] + \epsilon\chi^2\left[\mathbf{d}_a\frac{\partial P_c}{\partial t} + \mathbf{e}_a\left(\frac{\partial P_c}{\partial t}\right)^2\right],\end{aligned} \tag{97}$$

$$\begin{aligned}\langle \mathbf{v}_b \rangle = {} & \mathbf{L}_{ba}\cdot\mathbf{F}_a + \mathbf{L}_{bb}\cdot\mathbf{F}_b + \chi\mathbf{m}_b\frac{\partial P_c}{\partial t} \\ & + \epsilon\sum_{f=a}^{b}\sum_{f'=a}^{b} {}_3\mathbf{A}_{bff'}:\mathbf{F}_{f'}\mathbf{F}_f + \epsilon\chi\sum_{f=a}^{b}\left[\mathbf{B}_{bf}\cdot\frac{\partial \mathbf{F}_f}{\partial t}\right. \\ & \left. + \mathbf{C}_{bf}\cdot\mathbf{F}_f\frac{\partial P_c}{\partial t}\right] + \epsilon\chi^2\left[\mathbf{d}_b\frac{\partial P_c}{\partial t} + \mathbf{e}_b\left(\frac{\partial P_c}{\partial t}\right)^2\right].\end{aligned} \tag{98}$$

One may note that it is only the coefficients involving the time rate of change of the forces (the coefficients multiplied by χ) that require an independent measurement of the saturation moment $\partial \mathbf{r}_a/\partial t$ in order to be experimentally determined.

These are complicated unwieldy laws. Since for practical earth problems the order ϵ contributions will commonly be neglected, we elect to address here only the symmetry properties of the ϵ^0 contributions. It will be demonstrated that $\mathbf{L}_{ab} = \mathbf{L}_{ba}^T$, $\mathbf{L}_{aa} = \mathbf{L}_{aa}^T$, and $\mathbf{L}_{bb} = \mathbf{L}_{bb}^T$. Although the ϵ^1 symmetry properties are not considered, it will be demonstrated that the flux that is quadratic in the pressure gradients violates reciprocity.

Before addressing the tensorial symmetries, we begin by noting that $\mathbf{m}_b = -\mathbf{m}_a$. We have stated earlier that the $\mathbf{m}_f$ vanish in the absence of saturation gradients. These coefficients control the flows excited by a uniform change in the capillary pressure throughout a sample. In the presence of a saturation gradient, there will always be more meniscii on one side of a sample (say the low-saturation side) than on the other. So if P_c increases uniformly, there tends to be more influx of the nonwetting fluid a on the low-saturation side than on the high-saturation side resulting in a net average flow $\langle \mathbf{v}_a \rangle$ throughout the sample given by $\mathbf{m}_a \partial P_c/\partial t$. At the same time there will also be an oppositely directed flow $\langle \mathbf{v}_b \rangle$, and because there are no macroscopic-pressure gradients driving such incompressible flow, fluid conservation requires that $\langle \mathbf{v}_b \rangle = -\langle \mathbf{v}_a \rangle$ or, equivalently, $\mathbf{m}_b = -\mathbf{m}_a$.

A. Reciprocity of the linear laws

In a companion paper [6], we show how Onsager theory may be used to address the reciprocity question for this and other two-phase flow problems. Here, we use a classical argument that exploits nothing but the self-adjoint nature of the ϵ^0 Stokes equations and that is nearly identical to the familiar wave-field reciprocity arguments used in electromagnetic [14] and elastodynamic [15] theory. Using similar arguments, Pride [16] has treated the reciprocity of the electrokinetic transport equations while Flekkøy [17] has treated certain problems in hydrodynamic dispersion. Auriault [9] has addressed the symmetries using a variational form of the argument.

We begin with the relation between the ''cross'' coefficients $\mathbf{L}_{ab}$ and $\mathbf{L}_{ba}$. Let us define α flow fields to be those created when $\mathbf{F}_a \neq \mathbf{0}$ and $\mathbf{F}_b = \mathbf{0}$ and β fields to be those when $\mathbf{F}_b \neq \mathbf{0}$ and $\mathbf{F}_a = \mathbf{0}$. Throughout what follows, we keep P_c = const. Consider the following scalar products involving such α and β fields:

$$\begin{aligned} \mathbf{v}_a^\beta \cdot [\nabla \cdot \boldsymbol{\tau}_a^\alpha + \mathbf{F}_a = 0] \quad \text{in} \quad \Omega_{ao}, \\ \mathbf{v}_a^\alpha \cdot [\nabla \cdot \boldsymbol{\tau}_a^\beta = 0] \quad \text{in} \quad \Omega_{ao}, \end{aligned} \tag{99}$$

$$\begin{aligned} \mathbf{v}_b^\alpha \cdot [\nabla \cdot \boldsymbol{\tau}_b^\beta + \mathbf{F}_b = 0] \quad \text{in} \quad \Omega_{bo}, \\ \mathbf{v}_b^\beta \cdot [\nabla \cdot \boldsymbol{\tau}_b^\alpha = 0] \quad \text{in} \quad \Omega_{bo}. \end{aligned} \tag{100}$$

Upon using the identity $\mathbf{v} \cdot (\nabla \cdot \boldsymbol{\tau}) = \nabla \cdot (\boldsymbol{\tau} \cdot \mathbf{v}) - \nabla \mathbf{v} : \boldsymbol{\tau}^T$, noting that $\boldsymbol{\tau} = \boldsymbol{\tau}^T$, and adding, we obtain

$$\begin{aligned} \mathbf{F}_a \cdot \mathbf{v}_a^\beta = \nabla \cdot [\boldsymbol{\tau}_a^\beta \cdot \mathbf{v}_a^\alpha - \boldsymbol{\tau}_a^\alpha \cdot \mathbf{v}_a^\beta] + \nabla \mathbf{v}_a^\beta : \boldsymbol{\tau}_a^\alpha \\ - \nabla \mathbf{v}_a^\alpha : \boldsymbol{\tau}_a^\beta \quad \text{in} \quad \Omega_{ao}, \\ \mathbf{F}_b \cdot \mathbf{v}_b^\alpha = \nabla \cdot [\boldsymbol{\tau}_b^\alpha \cdot \mathbf{v}_b^\beta - \boldsymbol{\tau}_b^\beta \cdot \mathbf{v}_b^\alpha] + \nabla \mathbf{v}_b^\alpha : \boldsymbol{\tau}_b^\beta \\ - \nabla \mathbf{v}_b^\beta : \boldsymbol{\tau}_b^\alpha \quad \text{in} \quad \Omega_{bo}. \end{aligned} \tag{101}$$

Now $\nabla \mathbf{v}_a^\beta : \boldsymbol{\tau}_a^\alpha = \nabla \mathbf{v}_a^\alpha : \boldsymbol{\tau}_a^\beta$ as can be verified using the explicit form $\boldsymbol{\tau} = -\pi \mathbf{I} + \eta[\nabla \mathbf{v} + (\nabla \mathbf{v})^T]$ along with $\nabla \cdot \mathbf{v} = \mathbf{0}$ and the fact that only the symmetric part of $\nabla \mathbf{v}$ contributes to the double-dot products.

Thus, upon integrating Eqs. (101) over their respective domains, using the divergence theorem, introducing macroscopic flow definitions such as $\langle \mathbf{v}_a^\beta \rangle = V^{-1} \int_{\Omega_{ao}} \mathbf{v}_a^\beta dV$, and noting that the ϵ^0 contributions of the transport laws (97) and (98) with P_c = const give

$$\mathbf{F}_a \cdot \langle \mathbf{v}_a^\beta \rangle = \mathbf{F}_a \cdot \mathbf{L}_{ab} \cdot \mathbf{F}_b, \tag{102}$$

$$\mathbf{F}_b \cdot \langle \mathbf{v}_b^\alpha \rangle = \mathbf{F}_b \cdot \mathbf{L}_{ba} \cdot \mathbf{F}_a, \tag{103}$$

we then obtain by subtraction

$$\begin{aligned} \mathbf{F}_a \cdot \mathbf{L}_{ab} \cdot \mathbf{F}_b - \mathbf{F}_b \cdot \mathbf{L}_{ba} \cdot \mathbf{F}_a \\ = E_a - E_b + \frac{1}{V} \int \frac{dx_o dy_o}{h_{xo} h_{yo}} \\ \times \hat{\mathbf{z}}_o \cdot [\boldsymbol{\tau}_a^\beta \cdot \mathbf{v}_a^\alpha - \boldsymbol{\tau}_a^\alpha \cdot \mathbf{v}_a^\beta + \boldsymbol{\tau}_b^\alpha \cdot \mathbf{v}_b^\beta - \boldsymbol{\tau}_b^\beta \cdot \mathbf{v}_b^\alpha]. \end{aligned} \tag{104}$$

The surface integrals over the rigid grain surfaces (that arise from the divergence theorem and are not shown) vanish because of the no-slip condition. The contributions E_a and E_b are the integrals over the external surface given by

$$E_a = \frac{1}{V} \int_{\partial E_a} \mathbf{n} \cdot [\boldsymbol{\tau}_a^\beta \cdot \mathbf{v}_a^\alpha - \boldsymbol{\tau}_a^\alpha \cdot \mathbf{v}_a^\beta] dS, \tag{105}$$

$$E_b = \frac{1}{V} \int_{\partial E_b} \mathbf{n} \cdot [\boldsymbol{\tau}_b^\alpha \cdot \mathbf{v}_b^\beta - \boldsymbol{\tau}_b^\beta \cdot \mathbf{v}_b^\alpha] dS. \tag{106}$$

We would like to argue that these external surface integrals are always zero. If the sample is required to have periodic boundary conditions, then these integrals vanish exactly. However, periodic boundary conditions are inconsistent with the presence of saturation gradients. The boundary contributions E_a and E_b will also vanish if we imagine that each of the pores lying on the entrance and exit faces are deformed so that they are each locally straight conduits. If we do this in such a manner that leaves both the total pore area on the faces and the total flux rates across the faces invariant (this is always possible), then the nature of the flow throughout the majority of the sample will not be affected if the sample is sufficiently large (as can be justified using Green's tensors). In each of the small straight entrance conduits, however, the integrands of both E_a and E_b vanish. Such an argument is similar to Saint Venant's principle in elasticity theory and only requires that the local pore reconstructions on ∂E are over length scales much smaller than the size of the sample being considered.

Having ignored both E_a and E_b, we next introduce the boundary conditions (68) and (69) of the α and β problems into the remaining integrand over $z_o = 0$. It is seen that the integrand vanishes exactly so that

$$\mathbf{F}_a \cdot \mathbf{L}_{ab} \cdot \mathbf{F}_b - \mathbf{F}_b \cdot \mathbf{L}_{ba} \cdot \mathbf{F}_a = \mathbf{0}. \tag{107}$$

By systematically varying $\mathbf{F}_a$ and $\mathbf{F}_b$ to align with the principal directions of whatever coordinate system we are working in, we can finally conclude that $\mathbf{L}_{ab} = \mathbf{L}_{ba}^T$ as desired.

Similar arguments establish the symmetry of the tensors $\mathbf{L}_{aa}$ and $\mathbf{L}_{bb}$. We only sketch the argument for $\mathbf{L}_{aa}$ because the argument and conclusions for $\mathbf{L}_{bb}$ are identical. For the α problem, instead of considering the fields generated by $\mathbf{F}_a$ alone, we now consider the fields generated by two uniform force densities $\mathbf{F}_{a1}$ and $\mathbf{F}_{a2}$ that have arbitrary orientation and magnitude but that are both confined to the region Ω_{ao}. Defining α_1 and α_2 fields as those generated from $\mathbf{F}_{a1}$ and $\mathbf{F}_{a2}$, respectively, we form the following products:

$$\begin{aligned} \mathbf{v}_a^{\alpha 2} \cdot [\nabla \cdot \boldsymbol{\tau}_a^{\alpha 1} + \mathbf{F}_{a1} = 0] \quad \text{in} \quad \Omega_{ao}, \\ \mathbf{v}_a^{\alpha 1} \cdot [\nabla \cdot \boldsymbol{\tau}_a^{\alpha 2} + \mathbf{F}_{a2} = 0] \quad \text{in} \quad \Omega_{ao}, \end{aligned}$$

$$\begin{aligned} \mathbf{v}_b^{\alpha 2} \cdot [\nabla \cdot \boldsymbol{\tau}_b^{\alpha 1} = 0] \quad \text{in} \quad \Omega_{bo}, \\ \mathbf{v}_b^{\alpha 1} \cdot [\nabla \cdot \boldsymbol{\tau}_b^{\alpha 2} = 0] \quad \text{in} \quad \Omega_{bo}. \end{aligned}$$

If we add and use the identities established above, then

$$\begin{aligned} \mathbf{v}_a^{\alpha 2} \cdot \mathbf{F}_{a1} - \mathbf{v}_a^{\alpha 1} \cdot \mathbf{F}_{a2} = \nabla \cdot [\boldsymbol{\tau}_a^{\alpha 2} \cdot \mathbf{v}_a^{\alpha 1} - \boldsymbol{\tau}_a^{\alpha 1} \cdot \mathbf{v}_a^{\alpha 2}] \quad \text{in} \quad \Omega_{ao}, \\ \mathbf{0} = \nabla \cdot [\boldsymbol{\tau}_b^{\alpha 1} \cdot \mathbf{v}_b^{\alpha 2} - \boldsymbol{\tau}_b^{\alpha 2} \cdot \mathbf{v}_b^{\alpha 1}] \quad \text{in} \quad \Omega_{bo}. \end{aligned}$$

Each of these is then integrated over its respective domain, the divergence theorem applied, and the results added. The surface integrals over the grain surfaces again vanish, as do the integrals over the external surfaces. If the definition $\langle \mathbf{v}_a^{\alpha_i} \rangle = \mathbf{L}_{aa} \cdot \mathbf{F}_{ai}$ is introduced, where $i = 1,2$, we then arrive at

$$\begin{aligned} \mathbf{F}_{a2} \cdot \mathbf{L}_{aa} \cdot \mathbf{F}_{a1} - \mathbf{F}_{a1} \cdot \mathbf{L}_{aa} \cdot \mathbf{F}_{a2} \\ = \frac{1}{V} \int \frac{dx_o dy_o}{h_{xo} h_{yo}} \hat{\mathbf{z}}_o \cdot [\boldsymbol{\tau}_a^{\alpha 2} \cdot \mathbf{v}_a^{\alpha 1} - \boldsymbol{\tau}_a^{\alpha 1} \cdot \mathbf{v}_a^{\alpha 2} \\ + \boldsymbol{\tau}_b^{\alpha 1} \cdot \mathbf{v}_b^{\alpha 2} - \boldsymbol{\tau}_b^{\alpha 2} \cdot \mathbf{v}_b^{\alpha 1}]. \end{aligned}$$

Upon appealing to the boundary conditions of the α problem and using the fact that $\mathbf{F}_{a1}$ and $\mathbf{F}_{a2}$ are arbitrarily directed, we obtain the symmetry $\mathbf{L}_{aa}=\mathbf{L}_{aa}^{T}$. An identical argument and result holds for $\mathbf{L}_{bb}$.

Thus, the steady-state ($P_c=\text{const}$) linear laws controlling macroscopic flux of fluids a and b follow ''two-phase Darcy laws'' of the form

$$\begin{pmatrix}\langle\mathbf{v}_a\rangle\\ \langle\mathbf{v}_b\rangle\end{pmatrix}=\begin{pmatrix}\mathbf{L}_{aa} & \mathbf{L}_{ab}\\ \mathbf{L}_{ab}^{T} & \mathbf{L}_{bb}\end{pmatrix}\cdot\begin{pmatrix}\mathbf{F}_a\\ \mathbf{F}_b\end{pmatrix}. \tag{108}$$

It is important to remember that the reciprocity holds only if $\mathbf{L}_{ab}$ is measured at the same P_c value as $\mathbf{L}_{ba}$.

B. Breaking of reciprocity by the nonlinear laws

We now consider the ϵ^1 transport laws when $P_c=\text{const}$, which can be written

$$\langle\mathbf{v}_{f1}\rangle=({}_3\mathbf{L}_{faa}\cdot\mathbf{F}_a+{}_3\mathbf{L}_{fab}\cdot\mathbf{F}_b)\cdot\mathbf{F}_a+({}_3\mathbf{L}_{fba}\cdot\mathbf{F}_a+{}_3\mathbf{L}_{fbb}\cdot\mathbf{F}_b)\cdot\mathbf{F}_b. \tag{109}$$

If we write $\langle\mathbf{v}_{f1}\rangle=\langle\mathbf{v}_{f1}\rangle(\mathbf{F}_a,\mathbf{F}_b)$, then cross-coupling reciprocity can again be defined by considering whether $\mathbf{F}_a\cdot\langle\mathbf{v}_{a1}\rangle(0,\mathbf{F}_b)=\mathbf{F}_b\cdot\langle\mathbf{v}_{b1}\rangle(\mathbf{F}_a,0)$. Using the quadratic expressions (109), the cross-coupling reciprocity is thus defined by whether

$$\mathbf{F}_a\cdot{}_3\mathbf{L}_{abb}:\mathbf{F}_b\mathbf{F}_b=\mathbf{F}_b\cdot{}_3\mathbf{L}_{baa}:\mathbf{F}_a\mathbf{F}_a. \tag{110}$$

Since the coefficients ${}_3\mathbf{L}_{ff'f''}$ are pressure-gradient-independent material properties, it is immediately seen that for arbitrary values of the amplitudes $|\mathbf{F}_a|$ and $|\mathbf{F}_b|$, such reciprocity cannot be satisfied. In the presence of nonlinearity, such cross-coupling reciprocity is violated.

VIII. PRACTICAL SUMMARY AND DISCUSSION

We now summarize the laws in the form that they will most commonly be used in practical earth problems. The goal is to make as clear a comparison as possible between what we have learned here and the standard formulation as outlined in the Introduction. The two cases in which either $\chi=O(1)$ or $\chi=O(\epsilon)$ will be presented.

A. The $\chi=O(1)$ and $\epsilon=0$ laws

As stated previously, the condition $\chi=O(1)$ is typical of laboratory situations in which a highly permeable material experiences diffusion over small length scales. In this case, the macroscopic laws take the form

$$\nabla\cdot\langle\mathbf{v}_a\rangle=-\chi\mathcal{S}_0\frac{\partial(\overline{p}_a-\overline{p}_b)}{\partial t}, \tag{111}$$

$$\nabla\cdot\langle\mathbf{v}_b\rangle=\chi\mathcal{S}_0\frac{\partial(\overline{p}_a-\overline{p}_b)}{\partial t}, \tag{112}$$

$$\langle\mathbf{v}_a\rangle=-\mathbf{L}_{aa}\cdot\nabla\overline{p}_a-\mathbf{L}_{ab}\cdot\nabla\overline{p}_b+\chi\mathbf{m}_a\frac{\partial(\overline{p}_a-\overline{p}_b)}{\partial t}, \tag{113}$$

$$\langle\mathbf{v}_b\rangle=-\mathbf{L}_{ab}^{T}\cdot\nabla\overline{p}_a-\mathbf{L}_{bb}\cdot\nabla\overline{p}_b-\chi\mathbf{m}_a\frac{\partial(\overline{p}_a-\overline{p}_b)}{\partial t}. \tag{114}$$

This represents a complete set of equations for the two unknowns $\overline{p}_a$ and $\overline{p}_b$. All the coefficients ($\mathcal{S}_0$, $\mathbf{m}_f$, $\mathbf{L}_{ff'}$) are nonlinear functions of $P_c=\overline{p}_a-\overline{p}_b$ and all can be measured in a laboratory.

The nonstandard coefficient is $\mathbf{m}_a$, which, as discussed earlier, owes its existence to the presence of a saturation gradient. To estimate the importance of $\mathbf{m}_a$ relative to the standard Darcy-permeability terms requires, among other things, an estimate of how many meniscii are present per unit volume of material and this depends sensitively on the saturation history as well as the material type. We will not make such an estimate here. Of interest would be direct experimental measurements of $\mathbf{m}_a$. Although possible to perform, we are unaware of any such existing measurements.

A capillary-pressure law $P_c(\varphi_a)$ does not directly present itself in the development. Only the time derivative of the inverse of such a law has arrived,

$$\frac{\partial\varphi_a}{\partial t}=\chi\mathcal{S}_0(\overline{p}_a-\overline{p}_b)\frac{\partial(\overline{p}_a-\overline{p}_b)}{\partial t}. \tag{115}$$

If this expression is integrated in order to obtain a capillary-pressure law, an integration constant arrives that corresponds to the initial-state saturation of a given sample. Thus, there are always two distinct saturations that must be present in any proposed capillary-pressure law: (i) the initial-state saturation and (ii) the saturation changes induced by applied forces. These two contributions will have distinctly different gradients and so the common practice of replacing one of the two pressure gradients by $\nabla\varphi_a$ becomes a dangerous excercise. It is our preference that such substitutions be avoided and that the law of changes [Eq. (115)] be directly employed. We reemphasize that any laboratory measurements of $\mathcal{S}_0$ must be performed on samples with percolating fluids and over P_c ranges that do not migrate the contact lines.

We will not attempt to quantify the possible functional dependence of $\mathcal{S}_0=\mathcal{S}_0(P_c)$. However, de Gennes [3] has suggested that percolation theory might provide a universal scaling law of the form

$$\mathcal{S}_0=a(P_c-P_c^*)^{\delta}, \tag{116}$$

where the constant a and the percolation threshold P_c^* vary from one sample to the next while $\delta\approx-0.6$ (in three dimensions) is a universal constant. Our theory requires the contact lines to remain fixed as P_c changes so that saturation changes can only be due to stretching of the meniscii. Nonetheless, the grain surfaces in rocks are fractals [18] possessing a continuous spectrum of different-sized nooks and crannies into which, say, an oil meniscus could be pressed. Thus, fractal grain surfaces might be able to produce a saturation scaling law without significant migration of the initial contact lines. However, new contact lines would necessarily be created in such a process with accompanying hysteresis.

Such behavior is not allowed for in the simple scaling law of Eq. (116) nor in our theory. We thus leave such speculation to future work.

B. The $\chi = O(\epsilon)$ laws

The condition $\chi = \chi_o \epsilon$, where χ_o is $O(1)$, is now considered. Note that from the estimates of Eq. (41) we can define χ_o as

$$\chi_o = \frac{k}{\sigma \beta_a \ell_c^2}. \tag{117}$$

In order to estimate the magnitude of this dimensionless number, we need to know how the permeability k is related to the pore length ℓ_c. Thompson [18] has used percolation theory to obtain the following estimate:

$$k = \frac{\ell_c^2}{226F}, \tag{118}$$

in which ℓ_c is precisely the breakthrough radius in a mercury-invasion experiment while F is the electrical formation factor. The dimensionless product $226F$ is on the order of 10^4 in sandstones and, as such, should not be neglected even in order-of-magnitude estimates. Thompson presents data from 50 sedimentary rocks having permeabilities that span some six orders of magnitude to demonstrate the extraordinary validity of this relation. Assuming as earlier that $\sigma\beta_a \sim 10^{-8}$ m, we use Thompson's measurements of ℓ_c and F to obtain $\chi_o \lesssim 1$ for all 50 of Thompson's sandstones. Thus, the regime $\chi = O(\epsilon)$ is more than just an academic exercise. Indeed, it represents the more typical regime encountered in the earth.

The two-phase flow laws in this slow-diffusion regime are interesting because in order to model the saturation changes, terms through $O(\epsilon)$ must now be included,

$$\nabla \cdot \langle \mathbf{v}_a \rangle = -\chi_o \epsilon \mathcal{S}_0 \frac{\partial(\overline{p}_a - \overline{p}_b)}{\partial t}, \tag{119}$$

$$\nabla \cdot \langle \mathbf{v}_b \rangle = \chi_o \epsilon \mathcal{S}_0 \frac{\partial(\overline{p}_a - \overline{p}_b)}{\partial t}, \tag{120}$$

$$\langle \mathbf{v}_a \rangle = -\mathbf{L}_{aa} \cdot \nabla \overline{p}_a - \mathbf{L}_{ab} \cdot \nabla \overline{p}_b + \chi_o \epsilon \mathbf{m}_a \frac{\partial(\overline{p}_a - \overline{p}_b)}{\partial t} - \epsilon \sum_{f=a}^{b} \sum_{f'=a}^{b} {}_3\mathbf{A}_{aff'} : \nabla \overline{p}_{f'} \nabla \overline{p}_f, \tag{121}$$

$$\langle \mathbf{v}_b \rangle = -\mathbf{L}_{ab}^T \cdot \nabla \overline{p}_a - \mathbf{L}_{bb} \cdot \nabla \overline{p}_b - \chi_o \epsilon \mathbf{m}_a \frac{\partial(\overline{p}_a - \overline{p}_b)}{\partial t} - \epsilon \sum_{f=a}^{b} \sum_{f'=a}^{b} {}_3\mathbf{A}_{bff'} : \nabla \overline{p}_{f'} \nabla \overline{p}_f. \tag{122}$$

The difference between these equations and the standard formulation is now extreme. When $\chi = O(\epsilon)$, any estimates of how the saturation levels are changing that do not include the quadratic-force terms could easily be in error by an order of magnitude or more. Since the regime $\chi = O(\epsilon)$ seems to be the rule rather than the exception in the earth, we arrive at the unavoidable conclusion that to model saturation variations at points behind the macroscopic invasion front, quadratic-force Darcy laws must be used.

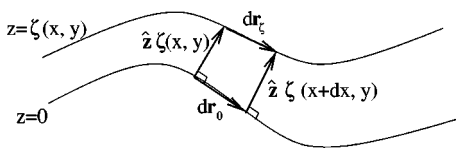

FIG. 5. Two neighboring points x and $x+dx$ on the initial interface $z=0$ and definition of the corresponding distance vectors.

ACKNOWLEDGMENTS

The authors are grateful to K. J. Måløy for valuable discussions and to Renaud Toussaint for pointing out an initial error in Sec. II A. E.G.F. acknowledges support by NFR, the Norwegian Research Council for Science and the Humanities, Grant No. 115846/420. This collaboration was made possible through a grant from the PICS program.

APPENDIX: PROPERTIES OF THE FLUID INTERFACE USING NORMAL COORDINATES

Before external forces are applied to the porous system, the fluid interface occupies a stable position and has curvilinear coordinates (x,y,z) attached to it where z defines the linear distance normal from the interface and x, y are orthogonal coordinates tangent to the surface. The length ds of an infinitesimal line element is given as

$$ds^2 = \left(\frac{dx}{h_x}\right)^2 + \left(\frac{dy}{h_y}\right)^2 + dz^2, \tag{A1}$$

where $h_x = h_x(x,y,z)$, $h_y = h_y(x,y,z)$, and $h_z = 1$ are the metrical coefficients of the coordinates. In this appendix, we are interested in characterizing the properties of the displaced surface

$$z = \zeta(x,y) \tag{A2}$$

using such ''normal coordinates.'' The goal is to define the mean curvature H, the normal vector $\mathbf{n}$, and the tangent vectors $\mathbf{t}$ in terms of the function ζ and the metrical coefficients h_x and h_y. Normal coordinates are meaningful (useful) only when the interface displacement ζ is much smaller than the initial radius of curvature of $z=0$; i.e., $|\zeta| \ll |2/H_o|$. If this condition is not met, then the coordinates can become multivalued and generally ill defined in the range of interest $0 < |z| < |\zeta|$.

Let $\mathbf{r}_\zeta$ denote the distance vector to points lying on the surface $z=\zeta$. We have $\mathbf{r}_\zeta = (x,y,\zeta)$ so that

$$d\mathbf{r}_\zeta = \frac{\partial \mathbf{r}_\zeta}{\partial x} dx + \frac{\partial \mathbf{r}_\zeta}{\partial y} dy. \tag{A3}$$

From Fig. 5 it is clear that by considering two neighboring points on $z=0$ at x and $x+dx$ separated by the distance $d\mathbf{r}_0 = \hat{\mathbf{x}} dx/h_x$, then

$$\zeta(x,y)\hat{\mathbf{z}} + d\mathbf{r}_\zeta = d\mathbf{r}_0 + \zeta(x+dx,y)\hat{\mathbf{z}}(x+dx,y) \tag{A4}$$

$$=\frac{dx}{h_x}\hat{\mathbf{x}}+\left(\zeta+\frac{\partial\zeta}{\partial x}dx\right)\left(\hat{\mathbf{z}}+\frac{\partial\hat{\mathbf{z}}}{\partial x}dx\right), \tag{A5}$$

where terms of $O(dx^2)$ have been neglected because dx is an infinitesimal. For curvilinear coordinates we have

$$\frac{\partial\hat{\mathbf{z}}}{\partial x}=-\frac{1}{h_x^2}\frac{\partial h_x}{\partial z}\hat{\mathbf{x}} \tag{A6}$$

so that

$$\frac{\partial\mathbf{r}_\zeta}{\partial x}=\frac{1}{h_x}\left(1-\frac{\zeta}{h_x}\frac{\partial h_x}{\partial z}\right)\hat{\mathbf{x}}+\frac{\partial\zeta}{\partial x}\hat{\mathbf{z}}, \tag{A7}$$

$$\frac{\partial\mathbf{r}_\zeta}{\partial y}=\frac{1}{h_y}\left(1-\frac{\zeta}{h_y}\frac{\partial h_y}{\partial z}\right)\hat{\mathbf{y}}+\frac{\partial\zeta}{\partial y}\hat{\mathbf{z}}, \tag{A8}$$

which are the two key vectors that will be needed in what follows. Note that the metrical coefficients and the derivatives with respect to z are all evaluated on the initial plane $z=0$ both here and throughout.

In differential geometry [19], the surface properties can be defined in terms of the coefficients of the two ''fundamental forms.'' The first fundamental form defines the infinitesimal distance along the surface and is thus written

$$d\mathbf{r}_\zeta\cdot d\mathbf{r}_\zeta=E dx^2+2F dx\,dy+G dy^2, \tag{A9}$$

where the coefficients are defined as

$$E=\frac{\partial\mathbf{r}_\zeta}{\partial x}\cdot\frac{\partial\mathbf{r}_\zeta}{\partial x}=\frac{1}{h_x^2}\left(1-\frac{\zeta}{h_x}\frac{\partial h_x}{\partial z}\right)^2+\left(\frac{\partial\zeta}{\partial x}\right)^2, \tag{A10}$$

$$F=\frac{\partial\mathbf{r}_\zeta}{\partial x}\cdot\frac{\partial\mathbf{r}_\zeta}{\partial y}=\frac{\partial\zeta}{\partial x}\frac{\partial\zeta}{\partial y}, \tag{A11}$$

$$G=\frac{\partial\mathbf{r}_\zeta}{\partial y}\cdot\frac{\partial\mathbf{r}_\zeta}{\partial y}=\frac{1}{h_y^2}\left(1-\frac{\zeta}{h_y}\frac{\partial h_y}{\partial z}\right)^2+\left(\frac{\partial\zeta}{\partial y}\right)^2. \tag{A12}$$

The second fundamental form of the surface $z=\zeta$ is defined $-d\mathbf{r}_\zeta\cdot d\mathbf{n}$, where $\mathbf{n}$ is the unit normal defined as

$$\mathbf{n}=\frac{\partial\mathbf{r}_\zeta/\partial x\times\partial\mathbf{r}_\zeta/\partial y}{|\partial\mathbf{r}_\zeta/\partial x\times\partial\mathbf{r}_\zeta/\partial y|}. \tag{A13}$$

Upon carrying out the cross products, we obtain

$$h_xh_yD\mathbf{n}=\left(1-\frac{\zeta}{h_x}\frac{\partial h_x}{\partial z}\right)\left(1-\frac{\zeta}{h_y}\frac{\partial h_y}{\partial z}\right)\hat{\mathbf{z}}-\left(1-\frac{\zeta}{h_y}\frac{\partial h_y}{\partial z}\right)h_x\frac{\partial\zeta}{\partial x}\hat{\mathbf{x}}-\left(1-\frac{\zeta}{h_x}\frac{\partial h_x}{\partial z}\right)h_y\frac{\partial\zeta}{\partial y}\hat{\mathbf{y}}, \tag{A14}$$

where the coefficient D is defined as

$$D^2\equiv EG-F^2. \tag{A15}$$

Thus, $\mathbf{n}$ has been defined solely in terms of h_x, h_y, and ζ. A change in $\mathbf{n}$ along $z=\zeta(x,y)$ is given by

$$d\mathbf{n}=\frac{\partial\mathbf{n}}{\partial x}dx+\frac{\partial\mathbf{n}}{\partial y}dy. \tag{A16}$$

Thus, with the second fundamental form written as

$$-d\mathbf{r}_\zeta\cdot d\mathbf{n}=e dx^2+2f dx\,dy+g dy^2, \tag{A17}$$

the coefficients e, f, and g are defined as

$$e=-\frac{\partial\mathbf{r}_\zeta}{\partial x}\cdot\frac{\partial\mathbf{n}}{\partial x}=\frac{\partial^2\mathbf{r}_\zeta}{\partial x^2}\cdot\mathbf{n}, \tag{A18}$$

$$f=-\frac{\partial\mathbf{r}_\zeta}{\partial x}\cdot\frac{\partial\mathbf{n}}{\partial y}=\frac{\partial^2\mathbf{r}_\zeta}{\partial x\partial y}\cdot\mathbf{n}, \tag{A19}$$

$$g=-\frac{\partial\mathbf{r}_\zeta}{\partial y}\cdot\frac{\partial\mathbf{n}}{\partial y}=\frac{\partial^2\mathbf{r}_\zeta}{\partial y^2}\cdot\mathbf{n}. \tag{A20}$$

We have used that $-d\mathbf{r}_\zeta\cdot d\mathbf{n}=\mathbf{n}\cdot d^2\mathbf{r}_\zeta$ because $\mathbf{n}\cdot d\mathbf{r}_\zeta=0$. It is easier to take a second derivative on $\mathbf{r}_\zeta$ than to differentiate $\mathbf{n}$. Thus, upon taking the second derivative we obtain the rather complicated expressions for e, f, and g,

$$De=\left(\frac{1}{h_y}-\frac{\zeta}{h_y^2}\frac{\partial h_y}{\partial z}\right)\frac{\partial\zeta}{\partial x}\left[\frac{1}{h_x^2}\frac{\partial h_x}{\partial x}+\frac{\partial}{\partial x}\left(\frac{\zeta}{h_x^2}\frac{\partial h_x}{\partial z}\right)+\frac{1}{h_x^2}\frac{\partial h_x}{\partial z}\frac{\partial\zeta}{\partial x}\right]-\left(\frac{1}{h_x}-\frac{\zeta}{h_x^2}\frac{\partial h_x}{\partial z}\right)^2\frac{\partial\zeta}{\partial y}\frac{h_y}{h_x^2}\frac{\partial h_x}{\partial y}+\left(\frac{1}{h_x}-\frac{\zeta}{h_x^2}\frac{\partial h_x}{\partial z}\right)\left(\frac{1}{h_y}-\frac{\zeta}{h_y^2}\frac{\partial h_y}{\partial z}\right)\times\left[\frac{\partial^2\zeta}{\partial x^2}+\frac{1}{h_x^2}\left(\frac{1}{h_x}-\frac{\zeta}{h_x^2}\frac{\partial h_x}{\partial z}\right)\frac{\partial h_x}{\partial z}\right], \tag{A21}$$

$$Df=\left(\frac{1}{h_y}-\frac{\zeta}{h_y^2}\frac{\partial h_y}{\partial z}\right)\frac{\partial\zeta}{\partial x}\left[\frac{1}{h_x^2}\frac{\partial h_x}{\partial y}+\frac{\partial}{\partial y}\left(\frac{\zeta}{h_x^2}\frac{\partial h_x}{\partial z}\right)\right]+\left(\frac{1}{h_x}-\frac{\zeta}{h_x^2}\frac{\partial h_x}{\partial z}\right)\frac{\partial\zeta}{\partial y}\left[\frac{h_x}{h_y^2}\left(1-\frac{\zeta}{h_x}\frac{\partial h_x}{\partial z}\right)\frac{\partial h_y}{\partial x}+\frac{1}{h_y^2}\frac{\partial\zeta}{\partial x}\frac{\partial h_y}{\partial z}\right]+\left(\frac{1}{h_x}-\frac{\zeta}{h_x^2}\frac{\partial h_x}{\partial z}\right)\left(\frac{1}{h_y}-\frac{\zeta}{h_y^2}\frac{\partial h_y}{\partial z}\right)\frac{\partial^2\zeta}{\partial x\partial y}, \tag{A22}$$

$$Dg=\left(\frac{1}{h_x}-\frac{\zeta}{h_x^2}\frac{\partial h_x}{\partial z}\right)\frac{\partial\zeta}{\partial y}\left[\frac{1}{h_y^2}\frac{\partial h_y}{\partial y}+\frac{\partial}{\partial y}\left(\frac{\zeta}{h_y^2}\frac{\partial h_y}{\partial z}\right)+\frac{1}{h_y^2}\frac{\partial h_y}{\partial z}\frac{\partial\zeta}{\partial y}\right]-\left(\frac{1}{h_y}-\frac{\zeta}{h_y^2}\frac{\partial h_y}{\partial z}\right)^2\frac{\partial\zeta}{\partial x}\frac{h_x}{h_y^2}\frac{\partial h_y}{\partial x}+\left(\frac{1}{h_y}-\frac{\zeta}{h_y^2}\frac{\partial h_y}{\partial z}\right)\left(\frac{1}{h_x}-\frac{\zeta}{h_x^2}\frac{\partial h_x}{\partial z}\right)$$

$$\times\left[\frac{\partial^2\zeta}{\partial y^2}+\frac{1}{h_y^2}\left(\frac{1}{h_y}-\frac{\zeta}{h_y^2}\frac{\partial h_y}{\partial z}\right)\frac{\partial h_y}{\partial z}\right]. \tag{A23}$$

The above results are exact to this point.

The *mean curvature* $H(\zeta)$ is defined at each point of the surface $z=\zeta(x,y)$ as $H(\zeta)\equiv R_x^{-1}+R_y^{-1}$, where R_x and R_y are the radius of curvatures in the x and y directions. It is expressible in terms of the coefficients D, E, F, G, e, f, g of the two fundamental forms as [19]

$$H(\zeta)=-\frac{(Eg-2Ff+Ge)}{D^2}. \tag{A24}$$

This expression is too complicated to write out explicitly in terms of h_x, h_y, and ζ.

However, in this paper, we only need the properties of the surfaces $z=0$ and $z=\epsilon\zeta$, where ϵ is taken as a very small parameter. When $z=0$ (i.e., $\zeta=0$), the above expressions give the normal and tangential vectors as

$$\mathbf{n}(0)=\hat{\mathbf{z}},\quad \mathbf{t}_x(0)=\hat{\mathbf{x}},\quad \mathbf{t}_y(0)=\hat{\mathbf{y}}, \tag{A25}$$

and the mean curvature as

$$H(0)\equiv H_o=-\frac{1}{h_x}\frac{\partial h_x}{\partial z}-\frac{1}{h_y}\frac{\partial h_y}{\partial z}. \tag{A26}$$

When $z=\epsilon\zeta$ and when terms only to first order in ϵ are kept, the normal and tangential vectors become

$$\mathbf{n}(\epsilon\zeta)=\hat{\mathbf{z}}-\epsilon\nabla\zeta,\quad \text{where}\quad \nabla\zeta=\hat{\mathbf{x}}h_x\frac{\partial\zeta}{\partial x}+\hat{\mathbf{y}}h_y\frac{\partial\zeta}{\partial y},$$

$$\mathbf{t}_x(\epsilon\zeta)=\hat{\mathbf{x}}+\epsilon h_x\frac{\partial\zeta}{\partial x}\hat{\mathbf{z}},\quad \mathbf{t}_y(\epsilon\zeta)=\hat{\mathbf{y}}+\epsilon h_y\frac{\partial\zeta}{\partial y}\hat{\mathbf{z}}, \tag{A27}$$

while the mean curvature becomes (after some algebra)

$$H(\epsilon\zeta)=H_o-\epsilon(\nabla^2\zeta+\xi^2\zeta). \tag{A28}$$

In the normal coordinates, the Laplacian is defined

$$\nabla^2\zeta=h_xh_y\left[\frac{\partial}{\partial x}\left(\frac{h_x}{h_y}\frac{\partial\zeta}{\partial x}\right)+\frac{\partial}{\partial y}\left(\frac{h_y}{h_x}\frac{\partial\zeta}{\partial y}\right)\right] \tag{A29}$$

while the coefficient ξ is defined

$$\xi^2\equiv\left(\frac{1}{h_x}\frac{\partial h_x}{\partial z}\right)^2+\left(\frac{1}{h_y}\frac{\partial h_y}{\partial z}\right)^2. \tag{A30}$$

These are the $O(\epsilon)$ results required in this paper. By setting $h_x=h_y=1$ throughout the above, we obtain the results for displacement from an initially flat interface.

[1] J. Bear, *Dynamics of Fluids in Porous Media* (Dover, New York, 1972).

[2] C. M Marle, *Multiphase Flow in Porous Media* (Gulf Publishing, Houston, 1981).

[3] P. de Gennes, Physico-Chem. Hydrodyn. **4**, 175 (1983).

[4] A. W. Adamson, *Physical Chemistry of Surfaces*, 5th ed. (Wiley Interscience, New York, 1990).

[5] P. Adler and H. Brenner, Annu. Rev. Fluid Mech. **20**, 35 (1988).

[6] E. G. Flekkøy and S. R. Pride, Phys. Rev. E **60**, 4130 (1999).

[7] W. G. Gray and S. M. Hassanizadeh, Water Resour. Res. **27**, 1847 (1991).

[8] S. Whitaker, Transp. Porous Media **1**, 105 (1986).

[9] J.-L. Auriault, Transp. Porous Media **2**, 45 (1987).

[10] J.-L. Auriault, O. Lebaigue, and G. Bonnet, Transp. Porous Media **4**, 105 (1989).

[11] S. R. Pride and J. G. Berryman, J. Mech. Phys. Solids **46**, 719 (1998).

[12] V. Frette, J. Feder, T. Jøssang, P. Meakin, and K. J. Måløy, Phys. Rev. E **50**, 2881 (1994).

[13] L. D. Landau and E. M. Lifshitz, *Theory of Elasticity* (Pergamon Press, New York, 1986), p. 6.

[14] J. A. Kong, *Electromagnetic Wave Theory* (Wiley, Interscience, 1990).

[15] A. E. H. Love, *A Treatise on the Mathematical Theory of Elasticity* (Dover, New York, 1944).

[16] S. Pride, Phys. Rev. B **50**, 15 678 (1994).

[17] E. G. Flekkøy, Phys. Fluids **9**, 3595 (1997).

[18] A. H. Thompson, A. J. Katz, and C. E. Krohn, Adv. Phys. **36**, 625 (1987).

[19] W. C. Graustein, *Differential Geometry* (Dover, New York, 1966).